

ARTICLE

Primary prostate cancer educates bone stroma through exosomal pyruvate kinase M2 to promote bone metastasis

Jinlu Dai¹, June Escara-Wilke¹, Jill M. Keller^{1,2}, Younghun Jung³, Russell S. Taichman³ , Kenneth J. Pienta⁴ , and Evan T. Keller^{1,2,5} 

Prostate cancer (PCa) metastasizes selectively to bone through unknown mechanisms. In the current study, we identified exosome-mediated transfer of pyruvate kinase M2 (PKM2) from PCa cells into bone marrow stromal cells (BMSCs) as a novel mechanism through which primary tumor-derived exosomes promote premetastatic niche formation. We found that PKM2 up-regulates BMSC CXCL12 production in a HIF-1 α -dependent fashion, which subsequently enhances PCa seeding and growth in the bone marrow. Furthermore, serum-derived exosomes from patients with either primary PCa or PCa metastasis, as opposed to healthy men, reveal that increased exosome PKM2 expression is associated with metastasis, suggesting clinical relevance of exosome PKM2 in PCa. Targeting the exosome-induced CXCL12 axis diminished exosome-mediated bone metastasis. In summary, primary PCa cells educate the bone marrow to create a premetastatic niche through primary PCa exosome-mediated transfer of PKM2 into BMSCs and subsequent up-regulation of CXCL12. This novel mechanism indicates the potential for exosome PKM2 as a biomarker and suggests therapeutic targets for PCa bone metastasis.

Introduction

Bone metastasis is a common sequela of many metastatic cancers. In men with advanced prostate cancer (PCa), the skeleton is the most frequent metastatic target. Approximately 84% of men develop bone metastases; whereas, the most common site of soft tissue metastasis, the liver, has a much lower incidence (~65%) and is rarely seen in men who have not been heavily treated for their bone metastases (Shah et al., 2004). The mechanisms that favor PCa to develop clinically detectable bone metastases more frequently than soft tissue metastases are not well defined. Metastasis is a complex process that involves a cascade of multiple steps for the successful establishment of clinically impactful metastases. In broad terms, increased bone specificity may be due to increased seeding of metastatic cells to the bone versus soft tissue sites and/or the ability of the bone microenvironment to promote PCa growth more efficiently than soft tissue sites. These concepts reflect Stephen Paget’s “seed and soil” theory, which suggests that certain combinations of cancer cells and distant site microenvironments optimize the opportunity for cancer cells to grow (Paget, 1889). However, this theory does not require that the optimal microenvironment exist before tumor growth.

Accordingly, one strategy a tumor could exploit to promote metastasis is to alter the distant microenvironment to facilitate tumor cell seeding or tumor growth.

Several reports have demonstrated that exosomes released from the primary tumor can modify distant sites to promote metastases at these sites (Hood et al., 2011; Peinado et al., 2012; Costa-Silva et al., 2015). Exosomes are membrane-bound vesicles in a range of 30–120 nm that are synthesized within multivesicular bodies and released from cells upon fusion of the multivesicular body with the cell membrane (Mathivanan et al., 2010; Taylor and Gercel-Taylor, 2011; Ge et al., 2012). Exosomes contain a variety of biomolecules, including proteins, mRNA, long non-coding RNA (lncRNA), and microRNA (miRNA) that can impact cell functions at distant sites. Thus, exosomes from the primary tumor may be able to deliver biomolecules that alter a distant site so that it gains the ability to promote metastasis. This process is defined as creation of a “premetastatic niche.”

In the current study, we sought to determine if PCa-derived exosomes can promote bone metastasis by modulating the bone marrow microenvironment and to identify a mechanism through which this was achieved.

¹Department of Urology, Medical School, University of Michigan, Ann Arbor, MI; ²Unit for Laboratory Animal Medicine, University of Michigan, Ann Arbor, MI; ³Periodontics and Oral Medicine, School of Dentistry, University of Michigan, Ann Arbor, MI; ⁴Department of Urology, Brady Urological Institute, Johns Hopkins University, Baltimore, MD; ⁵BioInterfaces Institute, University of Michigan, Ann Arbor, MI.

Correspondence to Evan Keller: etkeller@umich.edu.

© 2019 Dai et al. This article is distributed under the terms of an Attribution–Noncommercial–Share Alike–No Mirror Sites license for the first six months after the publication date (see <http://www.rupress.org/terms/>). After six months it is available under a Creative Commons License (Attribution–Noncommercial–Share Alike 4.0 International license, as described at <https://creativecommons.org/licenses/by-nc-sa/4.0/>).

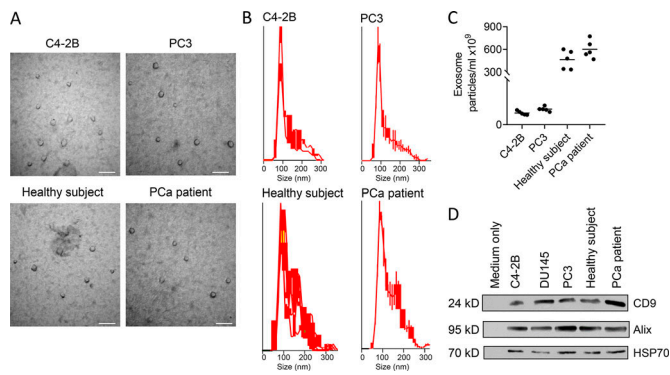


Figure 1. Characterization of exosomes after isolation. Exosomes were isolated from either cell culture conditioned-media or serum using density ultracentrifugation. **(A)** Electron micrographs of exosomes isolated from indicated samples. Exosomes of ~30–70 nm in diameter are shown. The scale bar indicates 100 nm. **(B)** Size distribution was determined using NTA (NanoSight). **(C)** Number of exosomes per ml of C4-2B- or PC3-conditioned media and serum from human subjects was determined using Nanosight. Results are shown as mean plus individual data points. **(D)** Western blot was performed for the indicated proteins. Measurements were performed on a set of two independent samples.

Results

PCa-derived exosomes promote tumor growth in mouse bone

Exosomes have been shown to have multiple functions on normal and cancer cells, which led us to evaluate if exosomes derived from PCa cells can impact the metastatic process. To evaluate whether PCa exosomes impact PCa progression, exosomes were harvested from PCa cell lines, and the exosomes were characterized. The exosomes isolated from the PC-3 and C4-2B PCa cells were composed of a discrete population based on electron microscopy; the majority of the population was in the size range of 60–150 nm, although the microvesicles ranged up to 300 nm, and they expressed CD9, ALIX, and HSP70 (Fig. 1). Taken together, these data confirm that this population was primarily exosomes, albeit with some nonexosomal microvesicles present (Théry et al., 2018). Mice were then pretreated with the exosomes followed by intracardiac (i.c.) injection (left ventricle) of PCa cells into the mice with continuous treatment of exosomes for 21 d. PCa exosomes induced an increase in the number of metastatic sites and the total tumor burden compared with vehicle (Fig. 2 A). Furthermore, if we used a different PCa cell line as the exosome donor or for implantation in mice, the results were similar, indicating that this effect was not cell specific (Fig. S1). To determine if exosomes from PCa patients impacted PCa metastasis, we repeated the PCa mouse model experiments using exosomes from the serum of healthy men versus those with primary PCa tumors. Exosomes from men with primary PCa tumors increased overall number of metastases and metastatic burden as opposed to those from healthy men (Fig. 2 B). Taken together, these results indicate that exosomes derived in the presence of cancer, as opposed to no cancer, confer a pro-metastatic activity.

An increased metastatic burden could be due to increased proliferation at the metastatic site and/or the enhanced ability of tumor cells to seed distant sites. To explore the latter

possibility, we pretreated mice with PCa exosomes for 4 d, injected PCa cells into the left cardiac ventricle, and then harvested marrow 24 h later to quantify PCa cells that seeded the bone marrow. Pre-treatment with PCa exosomes increased PCa cell seeding in the bone marrow by ~115% compared with vehicle treatment (Fig. 2 C). These data indicate that early differences in proliferation resulting from exosomes are unlikely to play a significant role in establishing differences between the treatment groups.

Exosomes may mediate their effect either directly on the cancer cells or indirectly through the microenvironment to create a premetastatic niche. To determine if the exosomes possessed functional activity directly on PCa cells, exosomes were isolated from both PCa cell lines and patients' sera, and PCa cells were incubated with the exosomes. The exogenous exosomes had no impact on PCa growth (Fig. S1, D and E).

The observation of no direct effects on PCa growth and invasion and previous reports that exosomes can modulate the microenvironment to promote tumor growth (Peinado et al., 2012; Ye et al., 2017) suggest that PCa exosomes impact PCa metastasis through the microenvironment. To determine if exosomes are able to target the microenvironment, we engineered cells to express fluorescently labeled exosomes. We initially injected these exosomes intravenously into mice and identified their presence in bone marrow stromal cells (BMSCs) at 24 h (Fig. 2 D). To specifically determine if exosomes from the primary tumor site can target distant sites, we injected PCa cells engineered to express fluorescent exosomes into the prostate of recipient mice and 3 wk later evaluated for exosomes in the bone marrow stroma. Exosomes were present in the bone marrow stroma at 3 wk after injection of the tumor cells (Fig. 2 E). To rule out if the fluorescence was due to cancer cells disseminating at that time point, we evaluated for the presence of human cells in the bone marrow using PCR for the Alu sequence as previously described (Shiozawa et al., 2011). Alu was not identified in any of the marrow samples, indicating no human cells were present at that time point (Fig. 2 F).

PCa has a predilection to metastasize to bone; however, it does metastasize to other sites (e.g., liver), albeit at a lower frequency. To determine if PCa exosomes targeted soft tissue sites in addition to bone, we injected fluorescently labeled PCa exosomes intravenously into mice and evaluated kidney, brain, liver, lung, and bone marrow for exosomes at 24 h. Exosomes were present in all tissues; however, they targeted the bone marrow stroma at a higher level than the other tissues on a per cell basis (Fig. 2 G).

Taken together, these results suggest that PCa exosomes do not have a direct effect on PCa cells but rather target and promote PCa progression indirectly through the distant target microenvironment, with selectivity toward targeting bone marrow. It is possible that the exosomes derived from the PCa cell line-conditioned media, once injected in vivo, are modified to have an impact directly on cancer cells, but this is unlikely as the exosomes from the PCa patients, which consist of in vivo-derived exosomes, did not have a direct effect on the tumor cells (Fig. S1 E), whereas, they did have an impact in vivo.

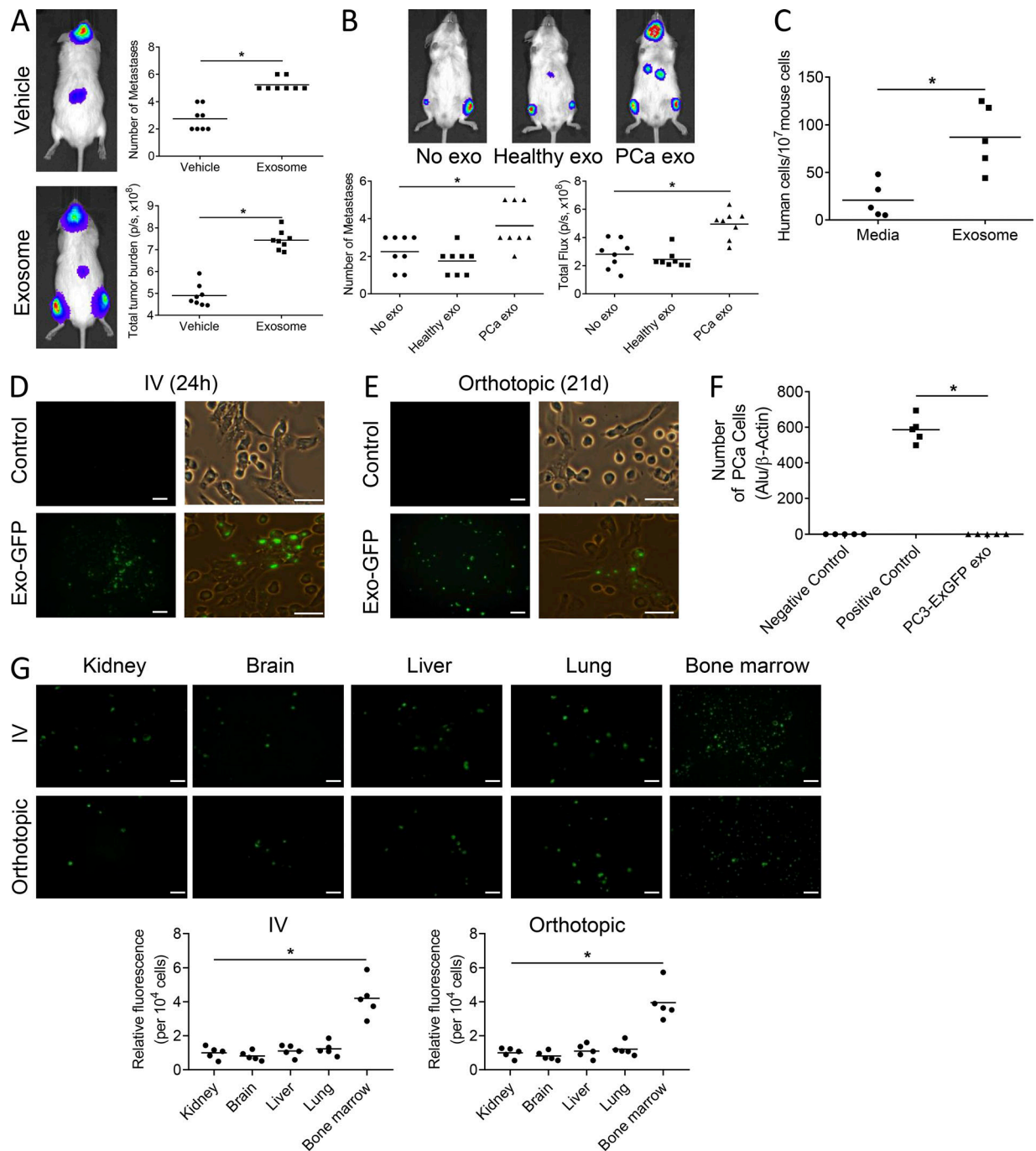


Figure 2. PCa-derived exosomes promote tumor growth in mouse bone. (A and B) SCID mice were pretreated with C4-2B–derived exosomes (A) or exosomes from healthy men versus those with primary tumors (B) or complete media for 4 d, followed by i.c. injection of PC3-luciferase cells with continuous treatment of exosomes for 21 d; $n = 8$ from 2 experiments. Number of metastases per mouse and total tumor burden were evaluated by BLI at the end of the study. Tumor burden and total flux are shown as photons/second (p/s). (C) qPCR analysis of Alu-positive cells in the bone marrow of SCID mice pretreated with exosomes and followed by i.c. injection of PC3-luciferase cells; $n = 5$ mice. (D) Representative fluorescence images of mouse bone marrow 24 h after i.v. tail vein injection of exosomes isolated from PC3 cells stably transduced with a lentivirus containing a fusion of CD63-GFP (PC3-ExGFP). Scale bar on left = 50 μm ; scale bar on right = 25 μm . (E) Representative fluorescence images of mouse bone marrow 3 wk after a one-time orthotopic injection of the PC3-ExGFP cells into the prostate of mice and establishment of orthotopic tumor. Scale bar on left = 50 μm ; scale bar on right = 25 μm . (F) PC3 cells stably transduced with a lentivirus containing a fusion of CD63-GFP (PC3-ExGFP) were injected into the prostates of male SCID mice. After 3 wk, bone marrows were harvested and subjected to qPCR analysis for Alu to determine the number of PCa cells in the bone marrow. Marrow without PCa cells and marrow with a known number of spiked-in PCa cells were used as negative and positive controls, respectively; $n = 5$ mice. (G) Left: Representative fluorescence images of the indicated tissues 24 h after i.v. tail vein injection of exosomes isolated from PC3-ExGFP cells or 3 wk after orthotopic injection of PC3-ExGFP cells. Scale bar = 50 μm . Right: Total fluorescence was measured and normalized to 10^4 cells; $n = 5$ mice. Data are shown as mean plus individual data points. *, $P \leq 0.05$ as determined by Student's *t* test (A and C) or ANOVA with Fisher's least significant difference (B, F, and G). In some cases, exosomes is abbreviated as exo.

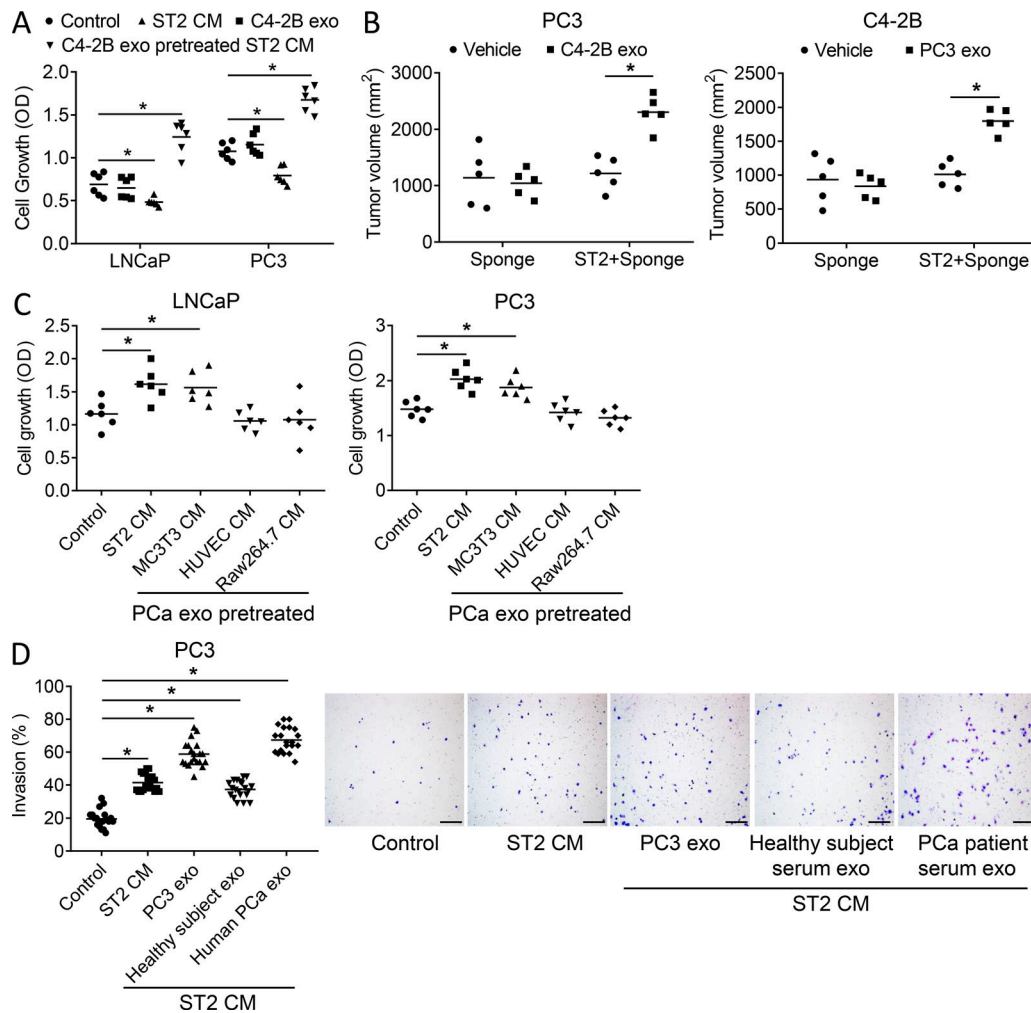


Figure 3. PCA-derived exosomes educate bone stromal cells to increase PCA tumor cell proliferation and invasion. (A) Proliferation of LNCaP and PC3 cells treated with fresh media, exosomes derived from C4-2B cells, ST2 cell-conditioned media, or conditioned media from ST2 cells treated with C4-2B exosomes for 48 h. Data from two experiments are shown. (B) Tumor volume on the flanks of SCID mice that had subcutaneous implantation of a collagen sponge loaded with either PC3 or C4-2B cells mixed with or without ST2 cells at 6 wks after implant; $n = 5$ mice. (C) Proliferation of LNCaP and PC3 cells treated with fresh media or conditioned media from ST2 cells, differentiated MC3T3 cells, HUVEC, or differentiated Raw264.7 cells pretreated with C4-2B exosomes for 48 h. Data from two experiments are shown. (D) Representative images of invasion and quantification results of PC3 treated with fresh media control, ST2 cell-conditioned media, or conditioned media from ST2 cells pretreated with exosomes isolated from PC3 cells or from healthy subject serum or from PCA patient serum. Scale bar = 150 μm . Data are shown as mean plus individual data points. *, $P \leq 0.05$ as determined by ANOVA with Fisher's least significant difference.

PCA-derived exosomes educate bone stromal cells to increase PCA tumor cell proliferation and invasion

To investigate if exosomes promote PCA progression indirectly through the microenvironment, we evaluated the extent to which exosomes alter the ability of BMSCs to influence PCA cell growth. As before, PCA exosomes had no direct effect on PCA cells; however, conditioned media from untreated stromal cells inhibited PCA cell growth (Fig. 3 A; and Fig. S2, A and B). In contrast, conditioned media from stromal cells pretreated with exosomes (derived from either PCA cells or PCA patients' serum) increased PCA cell growth (Fig. 3 A and Fig. S2), indicating that exosomes alter the stromal cells to promote PCA growth. To further explore this possibility, we subcutaneously implanted PCA cells on collagen sponges that had either no stromal cells or stromal

cells in opposite flanks of mice, and then treated the mice with either vehicle or PCA exosomes. Neither exosomes alone nor stromal cells alone impacted PCA growth, whereas in the stromal cell-laden sponges, exosomes induced PCA growth (Fig. 3 B). These results provide in vivo evidence that exosomes modulate stromal cells to promote PCA growth.

To determine if the exosome-mediated impact on stromal cells was specific to fibroblastic stroma or extended to other bone marrow cellular constituents, we examined the ability of PCA exosomes to impact the ability of endothelial, osteoblast, and osteoclast precursor cells to modulate PCA growth. Exosomes had the most potent effects in the fibroblastic stromal cells, followed by osteoblasts, and had no impact on endothelial cells or osteoclasts (Fig. 3 C).

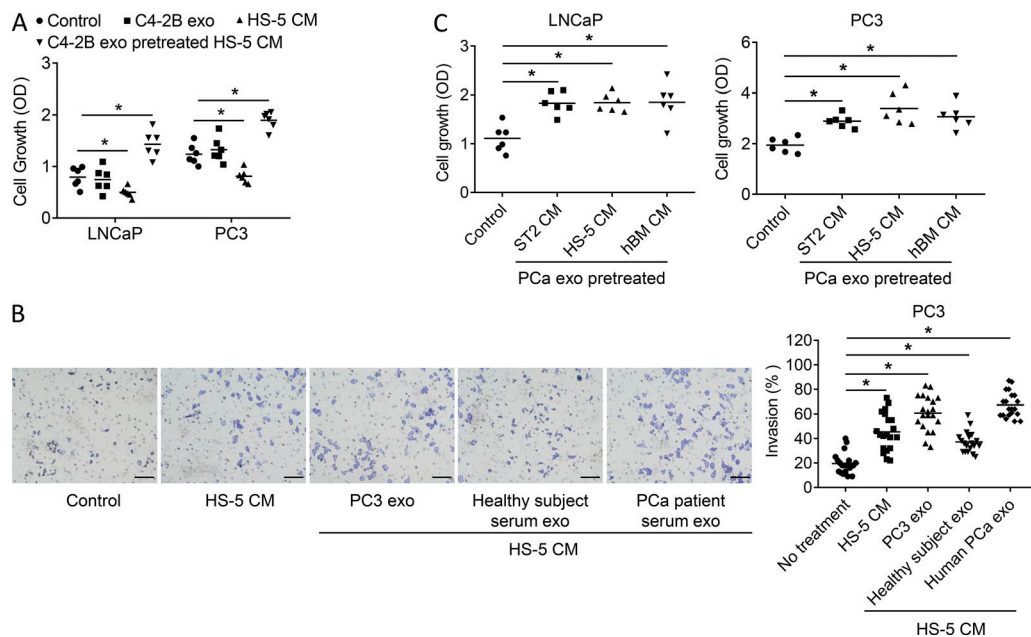


Figure 4. PCa-derived exosomes educate human BMSCs to increase PCa tumor cell proliferation and invasion. (A) Growth of LNCaP and PC3 cells treated with fresh media (control), exosomes derived from C4-2B cells, ST2 cell conditioned media, or conditioned media from ST2 cells treated with C4-2B exosomes. Data from two experiments are shown. **(B)** Representative images of invasion and quantification results of PC3 cells treated with either fresh media control, HS-5 cell-conditioned media, or conditioned media from HS-5 cells pretreated with exosomes isolated from PC3 cells or from healthy subject serum or PCa patient serum. Data from two experiments are shown. Scale bar = 70 μ m. **(C)** Growth of LNCaP and PC3 cells treated with fresh media (control), conditioned media from the ST-2 cells, HS-5 cells, or unprocessed human bone marrow that were treated with C4-2B-derived exosomes. Results are shown as mean plus individual data points. Data from two experiments are shown. *, $P \leq 0.05$ as determined by ANOVA with Fisher's least significant difference. hBM, human bone marrow; exo, exosome.

To determine if exosome-mediated modulation of stromal cells extends to other aspects of PCa progression, we evaluated their impact on the invasive properties of PCa cells. Stromal cell-conditioned media alone promoted PCa invasion; however, conditioned media from stromal cells pretreated with PCa cell exosomes further increased the invasive ability of PCa cells (Fig. 3 D). Furthermore, pretreatment of stromal cells with exosomes from healthy subjects increased invasion; however, invasion was increased even further if the stromal cells were pretreated with exosomes from PCa patients (Fig. 3 D).

As these studies were performed using a murine stromal cell line, we wanted to explore if these effects could extend to a human stromal cell line. Accordingly, we repeated several of the experiments using the HS-5 human BMSC line. Similar to the previous studies, both LNCaP-derived and PC-3-derived exosomes induced HS-5 to produce conditioned media (CM) that stimulated PCa growth (Fig. 4 A) and PCa invasive activity (Fig. 4 B). Additionally, we compared this effect to that of the ST2 cells and further evaluated the impact of PCa-derived exosomes on primary human bone marrow's ability to promote PCa growth. We found that both LNCaP-derived and PC-3-derived exosomes stimulated primary unprocessed human bone marrow and HS-5 cells at a level similar to that of ST2 cells (Fig. 4 C). These results indicate that the ability of PCa-derived exosomes is robust and provide further evidence of the human clinical relevance of this activity. Taken together, these data demonstrate the ability of exosomes to educate the marrow stroma to promote PCa progression.

PCa-derived exosomes increase pyruvate kinase M2 (PKM2) expression and C-X-C motif chemokine ligand 12 (CXCL12) production in stromal cells

The next challenge was to explore the mechanisms through which exosomes educate the marrow stroma toward a tumor-promoting phenotype. To examine for exosome-induced changes in the stromal cell proteome, ST2 cells were exposed to exosomes or vehicle, and then total cellular protein was collected and subjected to mass spectroscopy. Over 30 proteins that were present in both the untreated and treated cells were differentially expressed. The top 10 differentially expressed proteins are presented in Table 1. We focused on PKM2 both because it had one of the greatest magnitudes of change in expression (3.9-fold) and because of its pivotal role in cell biology. PKM2 is a glycolytic enzyme that plays a role in the glycolysis pathway and has several nonglycolytic functions, such as serving as a co-activator or protein kinase of various substrates (Tamada et al., 2012; Dong et al., 2016).

To validate that exosomes modulate stromal cell PKM2 expression, stromal cells were exposed to exosomes, and PKM2 protein expression was evaluated. PCa exosomes increased PKM2 protein expression in both ST2 cells and primary BMSCs (Fig. 5 A). Additionally, exosomes from PCa patients increased PKM2 protein expression in both ST2 cells and primary BMSCs (Fig. 5 B). In contrast to the increase of PKM2 protein in the stromal cells, PKM2 mRNA expression was not altered by exosomes in stromal cells (Fig. 5 C). These results suggest that exosomes do not induce transcription of PKM2 mRNA, but

Table 1. Protein profiling of C4-2B exosome-treated ST2 cells compared to untreated ST-2 cells

Proteins	Control ST2	Exo-treated ST2	Fold change
HS9B	0.1143	0.7894	6.91
ANXA2	0.1945	0.9693	4.98
TGM1	0.1538	0.7637	4.96
NID1	0.1384	0.6689	4.83
VIME	0.1712	0.7340	4.29
PKM2	0.1226	0.4780	3.90
LOXL3	0.1976	0.7637	3.86
G3P	0.1778	0.6237	3.51
CO1A1	0.1342	0.4599	3.43
PCOC1	0.1375	0.4674	3.40

rather transfer PKM2 protein from the exosome to the target cells and/or induce translation of PKM2 endogenously to the stromal cells. To determine whether or not exosomes induced PKM2 protein synthesis in the stromal cells, we treated stromal cells with the protein synthesis inhibitor cycloheximide (CHX). PCa-derived exosomes induced PKM2 levels in stromal cell-derived exosomes to similar levels in the absence or presence of CHX (Fig. 5 D), indicating that the increase is not dependent on protein synthesis. To provide further evidence that PKM2 was transferred from the human PCa cells to the murine stromal cells, we evaluated the PKM2 expression in stromal cells using antibodies that target human but not mouse PKM2. We found that treatment of stromal cells with exosomes containing human PKM2 (scramble control) increased human PKM2 expression in the stromal cells (Fig. 5 E, Human 1 and Human 2 immunoblots). There was no increase in human PKM2 when stromal cells were treated with exosomes derived from PCa cells in which PKM2 was knocked down. Furthermore, there was no increase observed in mouse PKM2 when stromal cells were treated with exosomes derived from PCa cells in which PKM2 was knocked down (Fig. 5 E, human and mouse immunoblot). Taken together, these results indicate that exosomes transfer PKM2 protein to the stromal cells as opposed to inducing PKM2 mRNA synthesis or protein synthesis.

Since it appears that exosomes transfer PKM2 to stromal cells, we wanted to assess if exosomes from PCa patients expressed PKM2. Accordingly, we harvested exosomes from the serum of healthy subjects, men with primary PCa (i.e., computerized tomography (CT) scan and bone scan negative), and men with PCa bone metastases (i.e., bone scan positive). Patient exosomes expressed PKM2 protein, and its expression increased with the presence of tumor and further with the presence of metastases (Fig. 5 F). These results provide clinically relevant evidence that exosomes contain PKM2, which could potentially increase PKM2 protein expression in exosome-targeted stroma.

We next wanted to determine if PKM2 could account for the exosomes' ability to modulate stromal cells to promote PCa growth. Our strategy was to knock down PKM2 expression in

PCa cells to create PKM2-deficient exosomes and test their ability to induce pro-tumorigenic activity. We first confirmed that knockdown of PKM2 resulted in exosomes deficient in PKM2 (Fig. 6 A and Fig. S3 A). We also found that knockdown of PKM2 did not impact exosome production (Fig. S3 B). We then determined if PKM2-deficient exosomes increased PKM2 in stromal cells. PKM2-deficient exosomes did not alter PKM2 protein expression in ST2 stromal cells (Fig. 6 B and Fig. S3 C) or MC3T3 stromal cells (Fig. S3 D). In addition to documenting that the PKM2 knockdowns were efficient, this finding further supports the earlier premise that PKM2 protein is transferred to the stromal cells as opposed to its synthesis being induced by exosomes. To determine if loss of PKM2 impacted tumor growth, we incubated cancer cell lines with conditioned media from stromal cells treated with exosomes deficient in PKM2. Decreased PKM2 expression in the PCa exosomes resulted in loss of the PCa exosomes' ability to induce PCa cell growth (Fig. 6 C).

We next wanted to determine if these *in vitro* findings extended to an impact on metastasis *in vivo*. Our strategy was to determine if PKM2 expression in primary tumors promoted metastasis. To accomplish this, we orthotopically implanted PCa cells with either knockdown of PKM2 or control shRNA vector. First, we determined if knockdown of PKM2 impacted primary orthotopic tumor growth. At 14 d after injection of tumor cells, a subset of mice from each group was euthanized, and tumor size was measured. There was no difference in orthotopic tumor size between the control scramble and PKM2 knockdown PCa cells (Fig. 6 D). PC-3 PCa luciferase-expressing cells were then injected via the *i.c.* route in the remaining animals of each group and an additional group that had not been previously injected orthotopically with tumor cells. The primary tumor cells were not luciferase expressing; thus, any cells expressing bioluminescence would be the *i.c.* injected PCa cells. At 3 wk after *i.c.* injection, mice were subjected to bioluminescent imaging (BLI), and the number of metastases and metastatic tumor burden were determined. The presence of primary orthotopic tumor (composed of the control scramble shRNA cells) increased the number of metastases and overall metastatic burden (Fig. 6, E and F). However, knockdown of PKM2 in the primary tumor cells partially diminished the ability of the primary tumor to increase the number of metastases and metastatic burden. These results demonstrate that primary prostate tumors promote metastasis and that PKM2 promotes the primary tumor's prometastatic ability. These results are consistent with the concept that primary tumors can promote metastasis, in part, through exosome PKM2.

PCa exosomes promote PCa tumor growth through CXCL12 from BMSCs induced by PKM2

To explore if PKM2 in PCa exosomes regulate stromal cells to produce soluble factors to promote PCa growth, a quantitative polymerase chain reaction (qPCR) array was used to evaluate for production of chemokines and cytokines from stromal cells treated with control or PKM2 knockdown PCa exosomes. PKM2 knockdown altered expression of several cytokines; however, expression of bone morphogenetic protein 4 (BMP-4) and CXCL12 were markedly decreased (Fig. 7 A). We initially

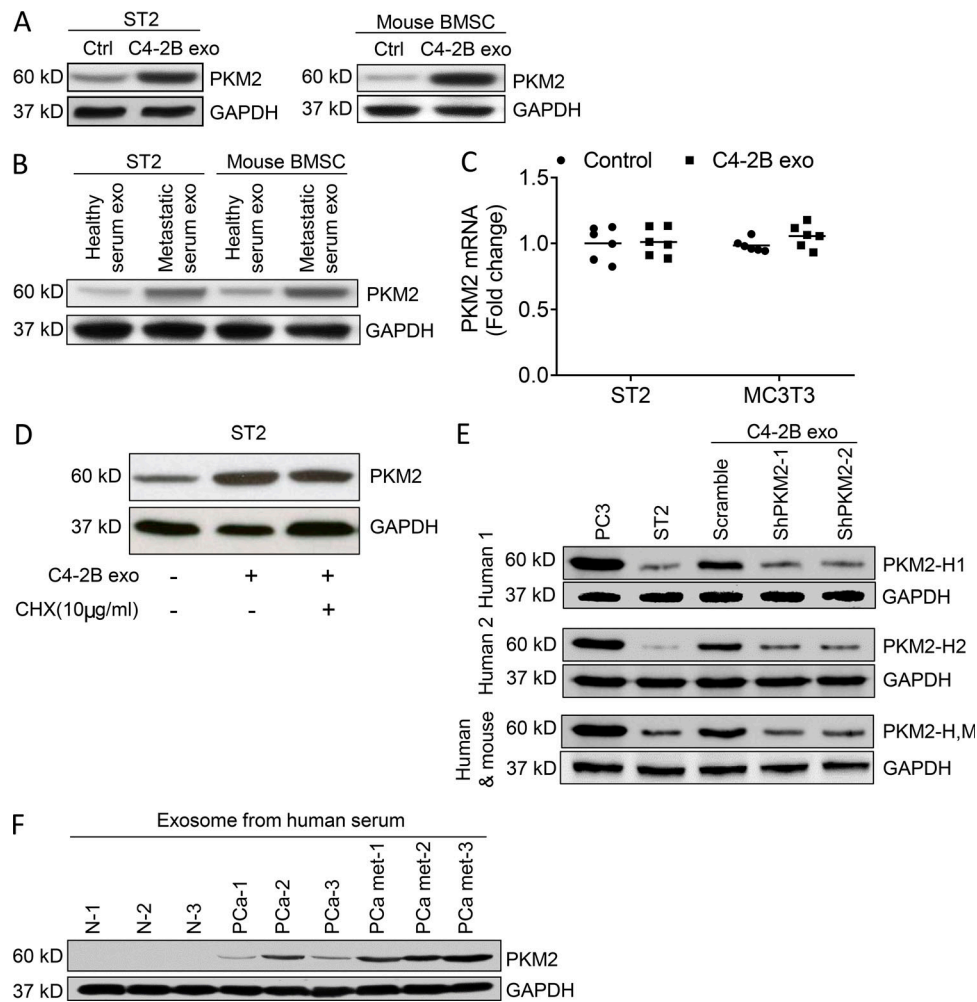


Figure 5. PCa-derived exosomes transfer PKM2 protein to BMSCs. (A) Western blot analysis of PKM2 in whole-cell lysate of ST2 cells and mouse BMSCs treated with control complete media (Ctrl) or C4-2B exosomes. (B) Western blot analysis of PKM2 in whole-cell lysate of ST2 cells and mouse BMSCs treated with exosomes isolated from the serum of healthy men or men with PCa bone metastases. (C) qRT-PCR analysis of PKM2 mRNA levels in ST2 and MC3T3 cells treated with C4-2B–derived exosomes or control media for 24 h. Data from two experiments are shown. Results are shown as mean plus individual data points. (D) Western blot analysis of PKM2 in the whole-cell lysate of ST2 cells exposed to exosomes from C4-2B cells or the protein synthesis inhibitor CHX as indicated. (E) Western blot analysis for PC3 cells, ST-2 cells, or ST-2 cells treated with PC3-derived exosomes from PC-3 cells treated with either scramble shRNA or PKM2 shRNA (two different targets). The blots were probed with human-specific antibodies (PKM2-H1 or PKM2-H2) or an antibody that recognizes both human and mouse PKM2 (PKM2-H,M). Experiments were repeated twice. (F) Western blot analysis of PKM2 in the exosomes isolated from the serum of healthy subjects (N), PCa patients with only localized disease (PCa), or patient with bone metastasis (PCamet).

validated the array findings. We found that PCa-derived exosomes induced CXCL12 mRNA and protein expression by over 13-fold, and knockdown of PKM2 in PCa exosomes decreased the ability of the PCa-derived exosomes to induce both CXCL12 mRNA and protein expression (Fig. 7 B). In contrast, we found that PCa-derived exosomes induced BMP-4 mRNA expression by less than onefold, although knockdown of PKM2 in PCa-derived exosomes decreased the ability of PCa-derived exosomes to induce BMP-4 mRNA expression (Fig. 7 C). Overall, these results indicate that PKM2 significantly increases CXCL12 production in stromal cells, whereas there is limited induction of BMP-4. Given the limited induction of BMP-4 expression and the previously described role of CXCL12 in increasing PCa bone metastasis through promoting proliferation and invasion (Taichman et al., 2000; Sun et al., 2003), we focused further investigation on CXCL12.

To determine if PCa exosome-educated stromal cells promoted PCa cell growth through CXCL12, we incubated PCa cells in conditioned media from PCa exosome-treated stromal cells in the absence or presence of AMD3100, which blocks the ability of CXCL12 to bind to its target, C-X-C chemokine receptor 4 (CXCR4). As previously observed, conditioned media from PCa-derived exosome-treated stromal cells increased PC3 and C4-2B cell growth and invasion; however, AMD3100 abrogated the induction of proliferation and invasion (Fig. 8, A and B [for PC-3 target cells] and Fig. S4, A and B [for C4-2B target cells]). These results indicate that CXCL12 contributes to the exosome-induced proliferative effect.

To examine if the stromal cell CXCL12-mediated PCa proliferative and invasive activity is dependent on PKM2 expression in the PCa exosomes that stimulate the stromal cells, PC3 cells were pretreated with AMD3100 or vehicle, followed by

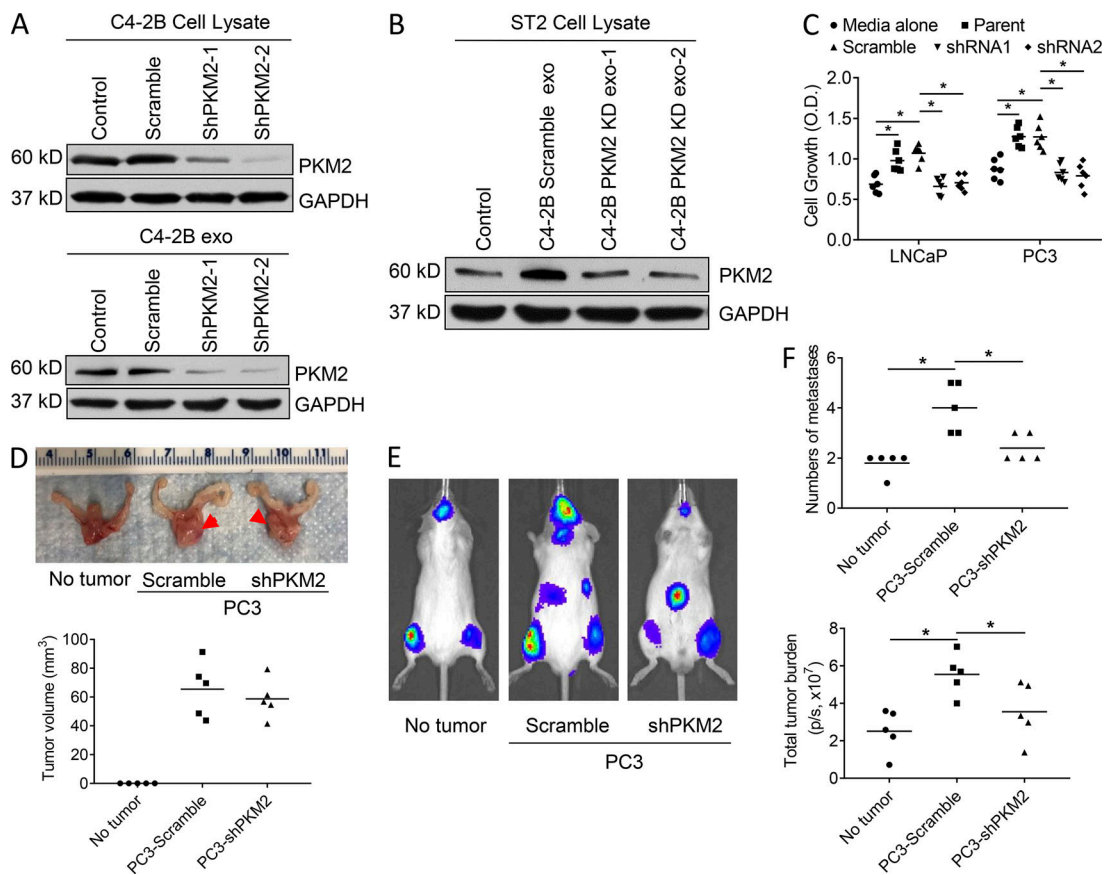


Figure 6. PCA-derived exosomes increase CXCL12 production in stromal cells through PKM2. (A) C4-2B cells were transduced with scramble, PKM2-shRNA-1, or PKM2-shRNA-2. Western blot analysis of PKM2 in the whole-cell lysate of the transduced C4-2B cells (upper) or exosomes isolated from the transduced C4-2B cells (lower). (B) Western blot analysis of PKM2 in the whole-cell lysate of ST2 stromal cells exposed to exosomes from C4-2B cells transduced with scramble, PKM2-shRNA-1, PKM2-shRNA-2, or control media. (C) Proliferation of LNCaP and PC3 cells exposed to exosomes from C4-2B cells transduced with scramble, PKM2-shRNA-1, or PKM2-shRNA-2 for 48 h. Each data point is derived from the mean of a triplicate sample, and results are reported as mean plus individual data points. (D) PC3-scrambled or PC3-shPKM2 knockdown cancer cells were injected into the prostates of mice; $n = 5$ mice. At 2 wk, mice were euthanized and prostates harvested. Upper: Tumor widths are indicated by arrowheads. Lower: Tumor volumes are indicated. (E and F) PC3-scramble or PC3-shPKM2 knockdown cancer cells were injected into the prostates of mice; $n = 5$ mice. These cells do not express luciferase. 2 wk later, PC3-luciferase cells were injected via the i.c. route. After an additional 3 wk, mice were imaged, and the number of metastases and total tumor burden were determined. Data are presented as mean and individual data points. *, $P \leq 0.05$ as determined by ANOVA with Fisher's least significant difference.

PCa-derived exosomes with or without PKM2 knockdown. As shown above, the conditioned media from stromal cells treated with PCa-derived exosomes increased PC3 cell proliferation and invasion, knockdown of PKM2 abrogated the ability of PCa-derived exosome-educated stromal cells to promote PCa cell growth, and AMD3100 blocked the ability of PCa-derived exosomes with intact PKM2 expression to educate stromal cells to promote PCa cell growth. However, the combination of using AMD3100 and PCa-derived exosomes with knockdown of PKM2 did not further inhibit proliferation or invasion compared with use of PCa-derived exosomes with PKM2 knockdown alone (Fig. 8, C and D). These experiments were repeated using C4-2B PCa cells as target cells, with similar results (Fig. S4, C and D). These results are consistent with PKM2 from PCa-derived exosomes modulating the production of CXCL12 in stromal cells to promote PCa growth and invasion.

Earlier in this study we had demonstrated that PCa-derived exosomes promote PCa cell seeding to the murine marrow. To determine if this activity was dependent on CXCL12, the mice

were pretreated with PCa-derived exosomes and either vehicle or AMD3100 administration. After 5 d, marrows were collected and subjected to PCR for human Alu sequences to quantify the human PCa cells in mouse bone marrow. PCa-derived exosomes increased PCa seeding to bone marrow, and AMD3100 diminished the seeding of PC-3 cells (Fig. 8 E).

To investigate if PCa-derived exosomes promote PCa metastasis in vivo through CXCL12, mice were pretreated with PCa exosomes for 5 d followed by i.c. injection of PC-3 PCa cells and administration of either vehicle or AMD3100. Exosome and AMD3100 administration were continued over a period of 4 wk, at which time the mice were euthanized. PCa-derived exosomes increased both the number of metastases and total metastatic burden of both C4-2B and PC-3 tumor cells, whereas AMD3100 inhibited these effects (Fig. 8, F and G). To further confirm that these results were mediated through the CXCL12:CXCR4 signaling axis, we knocked down CXCR4 expression in PC-3 cells (Fig. 8 H) and then repeated the evaluation for seeding and development of metastases. Similar to the AMD3100

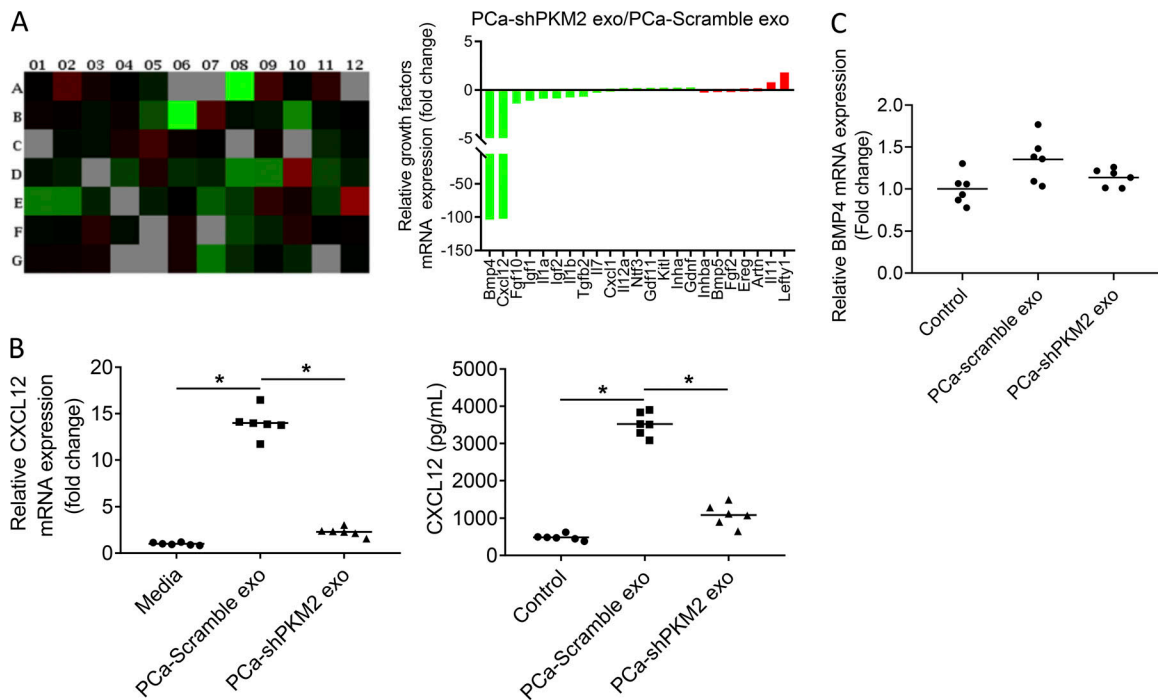


Figure 7. Exosomal PKM-2 promotes bone marrow stromal BMP-4 and CXCL12 expression. (A) Left: qPCR array of chemokines and cytokines in ST2 cells exposed to exosomes from C4-2B cells transduced with scramble or PKM2-shRNA. Right: Fold change of indicated cytokines induced in stromal cells by exosomes with PKM2 knockdown relative to control exosomes. This experiment was performed once. (B) Left: CXCL12 mRNA expression in ST2 cells exposed to exosomes from C4-2B cells transduced with scramble or PKM2-shRNA. Right: CXCL12 level in supernatant of ST2 cells exposed to exosomes from C4-2B cells transduced with scramble or PKM2-shRNA. (C) BMP4 mRNA expression in ST2 cells exposed to exosomes from C4-2B cells transduced with scramble or PKM2-shRNA. Results are shown as mean plus individual data points. *, $P < 0.05$ as determined by ANOVA with Fisher's least significant difference. These experiments were repeated two times.

administration, knockdown of CXCR4 in the PC-3 cells diminished exosome-induced seeding (Fig. 8 I) and the number of metastases and total metastatic burden (Fig. 8, J–L). Taken together, these results showed that exosomes contain PKM2, which can stimulate stromal cells to produce CXCL12 that promotes progression of PCa metastasis.

PCa-derived exosomes promote CXCL12 expression in stromal cells through induction of hypoxia-inducible factor 1 α (HIF-1 α) in a PKM2-dependent fashion

We next wanted to determine how exosomes induced CXCL12 expression. It has been previously shown that HIF-1 α promotes CXCL12 production (Ceradini et al., 2004; Martin et al., 2010). Thus, we first determined if exosomes promoted HIF-1 α expression and if this was dependent on PKM2. PC-derived exosomes stimulated HIF-1 α mRNA and protein expression in the ST2 stromal cell line and in primary murine BMSCs, whereas knockdown of PKM2 in the PCa-derived exosomes markedly decreased induction of HIF-1 α mRNA and protein expression (Fig. 9, A–C). These results indicate that PCa-derived exosomes promote HIF-1 α expression in a PKM2-dependent fashion. To determine if the exosome-induced HIF-1 α modulated CXCL12 expression, we knocked down HIF-1 α in stromal cells and treated the cells with exosomes to confirm loss of HIF-1 α expression (Fig. 9 D). We then treated stromal cells with C4-2B PCa-derived exosomes and observed that knockdown of HIF-1 α in the stromal cells markedly reduced the exosome-mediated induction of

CXCL12 mRNA (Fig. 9 E) and protein (Fig. 9 F). We repeated this experiment with PC3 PCa-derived exosomes and observed similar results (Fig. S5). Taken together, these data demonstrate that PCa-derived exosomes stimulate HIF-1 α expression in a PKM2-dependent fashion, which in turn induces CXCL12 expression.

Discussion

In the current study, we identify exosome-mediated transfer of PKM2 from PCa cells into BMSCs as a novel mechanism through which primary tumor-derived exosomes promote premetastatic niche formation. Our data suggest that primary PCa-derived exosomes increase PKM2 expression in BMSCs through transfer of PCa-derived PKM2 protein as opposed to up-regulating PKM2 production in BMSCs. PKM2, in turn, up-regulates BMSC CXCL12 production in a HIF-1 α -dependent fashion, which subsequently enhances PCa seeding and growth in the bone marrow. Furthermore, serum-derived exosomes from patients with either primary PCa or PCa metastasis, as opposed to healthy men, revealed that increased exosome PKM2 expression was associated with metastasis, suggesting both clinical relevance of exosome PKM2 and its potential as a biomarker. Finally, murine in vivo studies revealed that targeting the exosome-induced CXCL12 axis through either knockdown of its receptor, CXCR4, in PCa cells or through inhibition using AMD3100, a drug currently used in clinics for therapy of HIV,

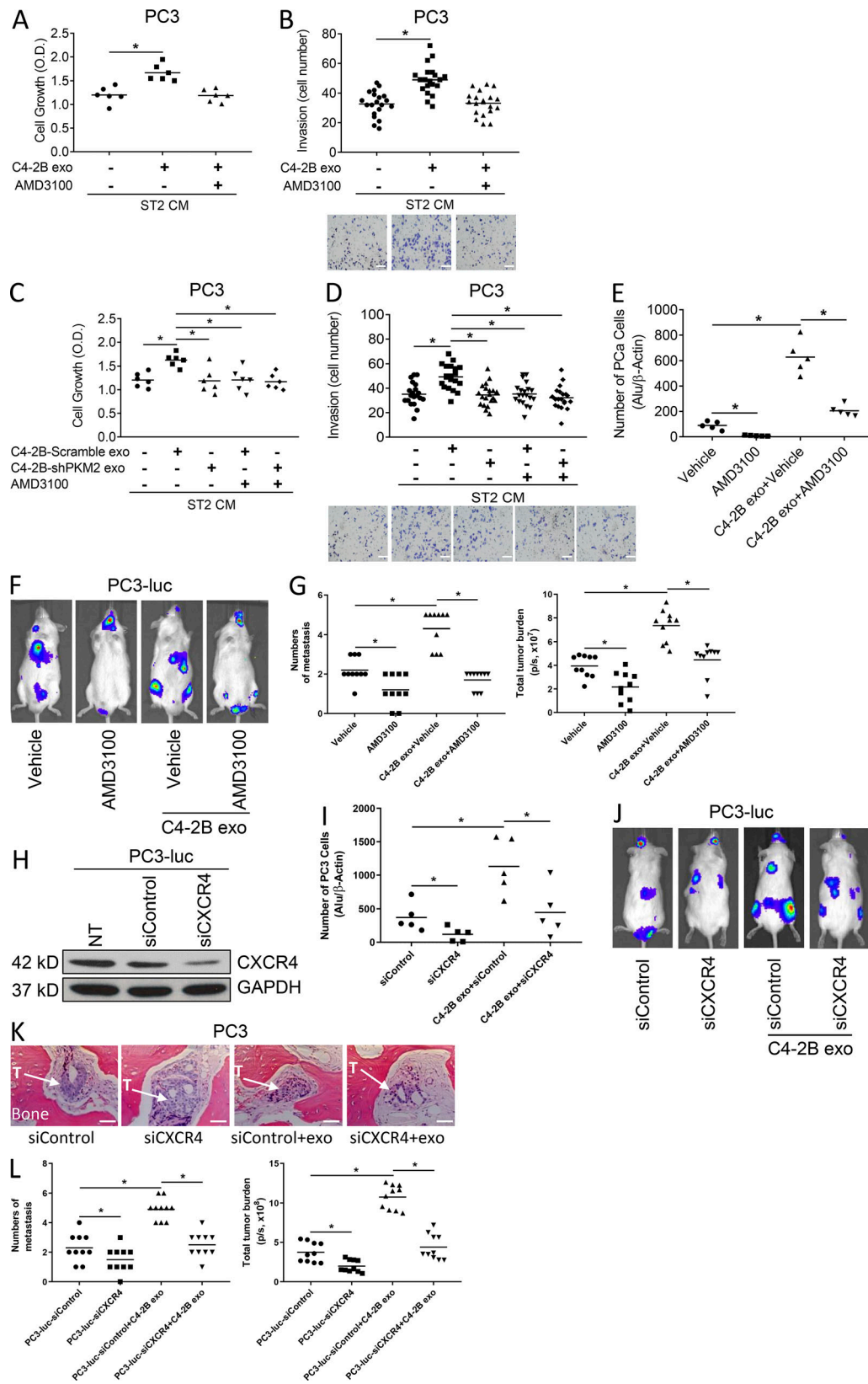


Figure 8. **PCa exosomes promote PCa tumor growth through CXCL12 from bone marrow cells induced by PKM2.** (A and B) Proliferation (A) and invasion (B) of PC3 cells exposed to exosomes from C4-2B cells with or without AMD3100 or control media for 48 h. Scale bar = 100 μ m. Data from two to three experiments are shown. (C and D) Proliferation (C) and invasion (D) of PC3 cells exposed to exosomes from C4-2B cells transduced with scramble or PKM2-shRNA with or without AMD3100 or control media for 48 h. Scale bar = 100 μ m. Data from two to three experiments are shown. (E) qPCR analysis of Alu-positive cell numbers in the bone marrow of SCID mice pretreated with exosomes from C4-2B cells with or without AMD3100 or AMD3100 or vehicle for

5 d followed with i.c. injection of PC3 cells; $n = 5$ mice. **(F)** Representative bioluminescent images of SCID mice pretreated with exosomes from C4-2B cells with or without AMD3100 or AMD3100 or vehicle for 5 d followed by i.c. injection of PC3-luciferase cells with continuous treatment of exosomes for 1 wk; $n = 10$ mice from two experiments. **(G)** Number of metastases per mouse and total tumor burden were evaluated by BLI for above mice. **(H)** Validation of CXCR4 knockdown by Western blot in PC3 cells. **(I)** qPCR analysis of Alu levels in the bone marrow of SCID mice pretreated with exosomes from C4-2B cells, followed by i.c. injection of PC3 cells treated with siCXCR4 or siControl; $n = 5$ mice. **(J)** Representative bioluminescent images of SCID mice pretreated with exosomes from C4-2B cells, followed by i.c. injection of PC3-luc cells treated with siControl, and continued exosome treatment for 1 wk; $n = 10$ mice from two experiments. **(K)** Representative histology from the indicated groups (hematoxylin and eosin stain). The trabecular bone is pink. "T" with arrow indicates location of tumor, often within stromal tissue. Scale bar = 100 μm . "exo" indicates the mice that had been treated with C4-2B exosomes. **(L)** Number of metastases per mouse and total tumor burden were evaluated by BLI for above mice. Data are shown as mean plus individual data points. *, $P \leq 0.05$ as determined by ANOVA with Fisher's least significant difference. These experiments were repeated two times.

diminished the ability of PCa-derived exosomes to promote bone metastasis. Taken together, our results demonstrate that primary PCa cells educate the bone marrow to create a premetastatic niche through primary PCa exosome-mediated transfer of PKM2 into BMSCs and subsequent up-regulation of CXCL12, a clinically targetable protein.

Multiple mechanisms have been suggested as mediators of crosstalk between PCa and bone (Yoneda and Hiraga, 2005; Suva et al., 2011; Ren et al., 2015). The majority of these mechanisms describe paracrine interactions of PCa cells producing soluble proteins that induce osteolytic (Zhang et al., 2001; Roato et al., 2008; Sabbota et al., 2010) or osteoblastic activity (Ortiz and Lin,

2012; Esposito et al., 2018; Shupp et al., 2018), which, in turn, results in altered bone remodeling and release of factors from the bone matrix that impact PCa growth. In addition to impacting PCa growth, the bone marrow has been shown to release the chemokine CXCL12 (also called stromal-derived factor-1), which acts as a chemoattractant to enhance seeding of PCa cells to the marrow (Taichman et al., 2002). Thus, crosstalk has been shown to occur locally, within the tumor microenvironment, and distantly. However, in the context of PCa, there are limited data regarding primary tumors creating a premetastatic niche. In the current study, we demonstrate that exosomes from the primary tumor can target the bone and have the ability to

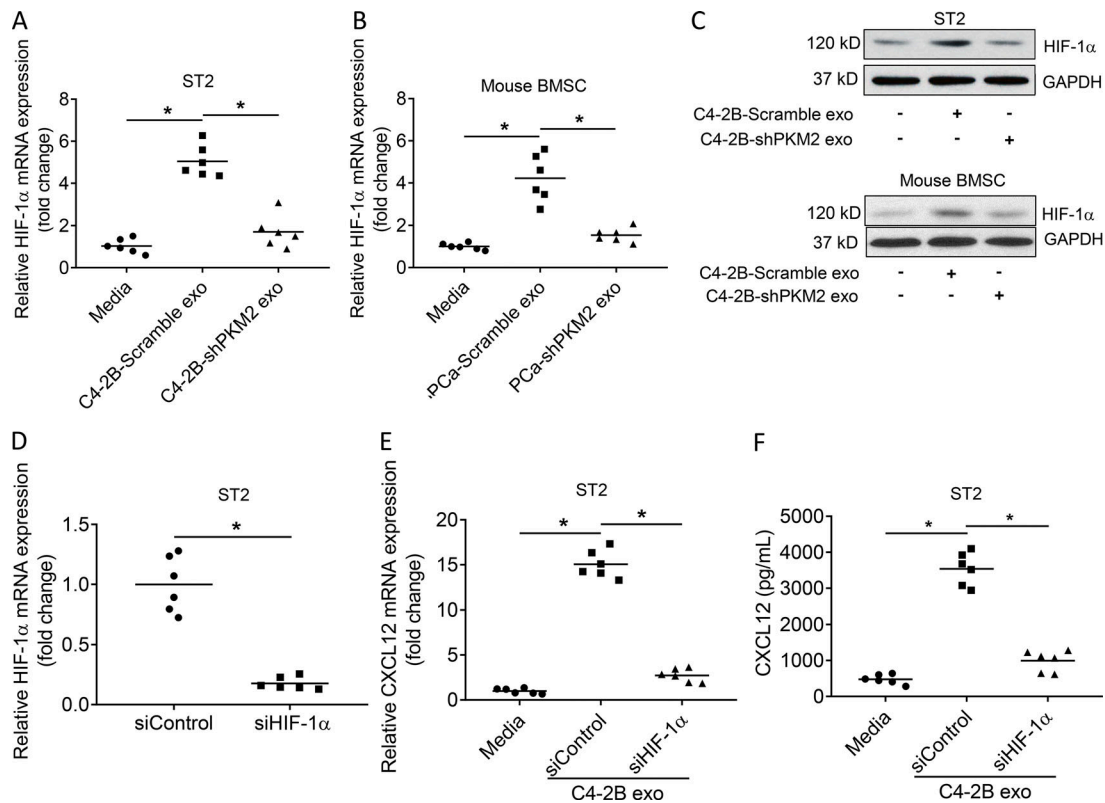


Figure 9. **PCa exosomes increase CXCL12 production in BMSCs through HIF-1 α induced by PKM2.** **(A and B)** HIF-1 α mRNA expression in ST2 cells (A) and mouse BMSCs (B) exposed to control media or exosomes from C4-2B cells transduced with Scramble or PKM2-siRNA. Data from two experiments are shown. **(C)** Western blot analysis of HIF-1 α in the whole-cell lysate of ST2 cells and mouse BMSCs exposed to exosomes from C4-2B cells transduced with Scramble, PKM2-siRNA, or control media. **(D)** HIF-1 α mRNA expression in ST2 cells treated with siControl or siHIF-1 α . Data from two experiments are shown. **(E)** CXCL12 mRNA expression in ST2 cells exposed to exosomes from C4-2B cells with siControl, siHIF-1 α , or control media. Data from two experiments are shown. **(F)** CXCL12 level in the supernatant of ST2 cells exposed to exosomes from C4-2B cells with siControl, siHIF-1 α , or control media. Data from two experiments are shown. Data are shown as mean and individual data points. *, $P \leq 0.05$ as determined by Student's t test (D) or ANOVA with Fisher's least significant difference (A, E, and F).

deliver a protein, PKM2, that can alter the bone microenvironment to promote growth of PCa metastases.

Exosomes have been recognized to transfer biomolecules, such as proteins, miRNA, and mRNA, to many different cells (Camussi et al., 2011; Dragomir et al., 2018; Jella et al., 2018). Initial studies demonstrating that exosomes from primary tumor could enhance metastasis include a report in which exosomes from primary melanoma were shown to target sentinel lymph nodes and enhance their ability to recruit metastasizing melanoma cells (Hood et al., 2011). Additionally, in a later study, primary melanoma exosomes were shown to educate the bone marrow stroma through increasing MET oncogene expression in stromal cells, which enhances metastasis to bone (Peinado et al., 2012). In terms of PCa, there are several studies regarding the potential of serum and urine exosomes as biomarkers (Valentino et al., 2017; Wani et al., 2017; Fujita and Nonomura, 2018; Lee et al., 2018; Panigrahi et al., 2018; Wang et al., 2018); however, there are limited functional studies that delineate if exosomes mechanistically impact PCa metastasis. In one study, exosomes containing miR-141-3p were shown to target osteoblasts and increase osteoblast activity (Ye et al., 2017). Although, the authors concluded in that study that exosome miR-141-3p enhanced osteoblastic metastasis, in that study, they injected mimic miR-141-3p miRNAs into the cancer cells that were then injected into the mice intratibially; thus, one may not conclude that the exosomes achieved their effect through altering the microenvironment or that there was any impact on tumor seeding. In another study, PCa-derived exosomes were shown to transfer $\alpha\text{v}\beta\text{6}$ integrin to monocytes, which enhanced their polarization to the M2 phenotype, which has been shown to enhance cancer progression (Lu et al., 2018). While this targeting is neither specific to metastasis in general (i.e., it would impact monocytes in primary tumor) nor the bone microenvironment specifically, it still provides a promising venue to explore as a therapeutic target. In addition to exosomes, reports of large (1–10 μm) microvesicles that were termed “prostate oncosomes” have been shown to contain a myriad of proteins, including active enzymes, and have the potential to target distant sites (Di Vizio et al., 2012). In the current study, we provide a novel mechanism through which primary tumor-derived exosomes target and alter the bone marrow microenvironment. Furthermore, this work provides several putative therapeutic targets including PKM2 and CXCL12.

PKM2 is an enzyme that catalyzes the conversion of phosphoenolpyruvate to pyruvate, which is the final step in the glycolytic pathway. It is expressed through an alternate splice from PKM precursor mRNA (pre-mRNA; Chen et al., 2010). PKM2 is highly expressed in many cancers and considered to contribute to the ability of cancer cells to preferentially use anaerobic glycolysis, even in the presence of ample oxygen, which is known as the Warburg effect (Luo and Semenza, 2011; Yang and Lu, 2013). In addition to its key role in the glycolytic pathway, it has been identified that PKM2 has nonglycolytic activity, including the ability to act as a transcriptional co-activator, a protein kinase, an angiogenic agent, and a differentiating agent (Iqbal et al., 2014; Wang et al., 2014; Warner et al., 2014; Dong et al., 2016). Of particular relevance to the

current report, PKM2 has been shown to enhance HIF-1 α -mediated transcription through acting as a co-activator (Luo and Semenza, 2011; Semenza, 2011; Azoitei et al., 2016). This sets the stage for HIF-1 α 's ability to promote CXCL12 production (Ceradini et al., 2004; Loh et al., 2009; Martin et al., 2010). These reports account for our finding that PKM2 induces CXCL12 in a HIF-1 α -dependent fashion.

Our study is the first, to our knowledge, to demonstrate that primary tumor-derived exosomes selectively target bone marrow versus soft tissue sites. The mechanism through which the exosomes selectively targeted marrow versus soft tissue sites is unclear. Several possibilities include that exosomes express specific proteins on their surface, derived from the PCa cells, that target the bone marrow stroma. Another possibility is that the blood flow in the marrow sinusoids, which is slower than that of blood vessels in soft tissue organs, may allow for more exposure time and interaction of exosomes with the marrow stroma. Further studies to explore this important question are warranted.

The current study demonstrates for the first time that exosome-mediated transfer of PKM2 from the exosomes to BMSCs promotes PCa bone metastasis, although primary cancer exosomes have been demonstrated to transfer biomolecules, including proteins, to other tissues. Additionally, we show that the exosomes induce CXCL12, a well-recognized promoter of PCa bone metastasis (Taichman et al., 2002; Papachristou et al., 2012), through a PKM2-mediated HIF1 α -dependent pathway. These results suggest a novel mechanism to account for the higher incidence of PCa bone metastases versus soft tissue metastases and provide a potential signaling pathway for targeting progression of bone metastasis.

In addition to the novel mechanisms of premetastatic niche formation described in the current report, we also identified that serum-derived exosome PKM2 was elevated in men with primary and metastatic PCa compared with men without PCa. These results are consistent with reports that indicate both PKM2 tumor expression (Desai et al., 2014; Mohammad et al., 2016; Chao et al., 2017; Zhu et al., 2017; Huang et al., 2018) and PKM2 blood levels (Fung et al., 2015; Croner et al., 2017; Rzechonek et al., 2017) are associated with a poor prognosis. We believe this is the first description of exosome PKM2 levels in the blood of cancer patients. Due to the small number of patients in the current study, these data are only suggestive, but provide the rationale to explore this in a larger cohort.

Overall, this work suggests a novel mechanism through which the primary tumor crosstalks with the bone microenvironment to establish a premetastatic niche and promote PCa bone metastatic progression. Taken together, our experiments demonstrate that tumor-derived exosome-mediated transfer of PKM2 is a critical mediator of modulating the bone marrow microenvironment to promote CXCL12 expression and progression of PCa bone metastasis.

Materials and methods

Cell culture

Human PCa cell lines LNCaP, DU145, and PC3 were obtained from the American Type Culture Collection (ATCC) and cultured

in RPMI 1640 (Invitrogen Co.) supplemented with 10% FBS and 1% penicillin-streptomycin (Life Technologies, Inc.). The C4-2B cell line, which is an LNCaP subline, was maintained in T medium (80% DMEM [Life Technologies, Inc.], 20% F12 [Invitrogen], 100 U/liter penicillin G, 100 µg/ml streptomycin, 5 µg/ml insulin, 13.6 pg/ml triiodothyronine, 5 µg/ml transferrin, 0.25 µg/ml biotin, and 25 µg/ml adenine) supplemented with 10% FBS. MC3T3-E1 (clone MC-4; kindly provided by Dr. Renny Franceschi, University of Michigan, Ann Arbor, MI) is a preosteoblast cell line derived from murine calvaria that, when treated with ascorbate, expresses osteoblast-specific markers and is capable of producing a mineralized matrix and was maintained in α -MEM containing 10% FBS and 1% penicillin-streptomycin (Life Technologies, Inc.). ST2 cells, a mouse BMSC line, were obtained from RIKEN Cell Bank and maintained in MEM Alpha (Invitrogen) supplemented with 10% FBS, 1% penicillin-streptomycin (Life Technologies, Inc.), and 2 mM L-glutamine (Invitrogen). The murine monocyte/macrophage-like cell line, RAW 264.7 (obtained from ATCC), commonly used as an osteoclast precursor cell line, was maintained in RPMI 1640 supplemented with 10% FBS, 1% penicillin-streptomycin, and 2 mM L-glutamine. HUVECs (obtained from ATCC) were maintained in EGM-2 medium (Lonza) containing 10% FBS and 1% penicillin-streptomycin. HS-5, a human bone marrow fibroblastic BMSC line, was obtained from ATCC and grown in DMEM (Life Technologies, Inc.), with 100 U/liter penicillin G and 100 µg/ml streptomycin supplemented with 10% FBS. All cultures were maintained at 37°C, 5% CO₂, and 100% humidity. Authentication of cell lines is performed every 6 mo using short tandem repeat profiling. All cells tested negative for mycoplasma.

Human samples

Human peripheral blood samples were obtained from control subjects and patients with histologically confirmed stage 1–4 PCa. Patients were either CT and bone scan negative for metastasis (defined as primary tumor only) or bone scan positive (defined as bone metastasis). Serum from the patients were stored at –80°C until used. All individuals provided informed consent for blood donation according to a protocol approved by the University of Michigan Institutional Review Board. Unprocessed human bone marrow was obtained commercially (Lonza). Procurement of the samples was approved by the University of Michigan Institutional Review Board.

Procurement of conditioned media

Cells were grown to 80% confluence in the appropriate complete medium containing 10% FBS in 10-cm tissue culture dishes. At this point, the medium was removed, and the cells were gently washed with PBS. Cells were treated with 100 µl PCa exosome (10⁹ particles/ml) in 10 ml of cell culture medium appropriate for the target PCa cell lines containing 0.5% FBS or the medium with exosomes as control. After 24 h, conditioned medium was collected, centrifuged at 1,000 *g* for 3 min to remove the cell debris, concentrated with Biomax centrifugal filter device (molecular weight cutoff: 10 kD; Millipore Corp.), and then frozen. At time of media collection, cells were counted, and CMs were normalized by adding media to a final volume to represent 1 × 10⁶ cells/ml.

Exosome isolation

PCa cells were cultured in media supplemented with 1% exosome-depleted FBS (SBI). After 24 h, cell culture media were harvested and centrifuged at 300 *g* at 4°C for 10 min to remove detached cells. Supernatant was collected and filtered through 0.2-µm nylon filters (Fisherbrand) to remove contaminating apoptotic bodies, microvesicles, and cell debris and then concentrated ~200 times using a Centricon Plus-70 centrifugal filter device with a 10 K NMWL (Millipore). Exosomes were then harvested by centrifugation at 100,000 *g* for 90 min (T-890 Rotor; Thermo Fisher Scientific) to pellet exosomes. The supernatant was carefully removed, and crude exosome-containing pellets were resuspended in 1 ml of ice-cold PBS. The exosome pellet was resuspended in 10 ml of PBS and collected by density ultracentrifugation at 100,000 *g* for 70 min as described below. The exosomes from human serum were isolated as described above.

To accomplish density centrifugation, the samples were diluted 1:10 in PBS after centrifugation at 20,000 *g* and then collected by ultracentrifugation (100,000 *g* for 70 min) on a 40% sucrose cushion. The floating exosome fraction was collected again by ultracentrifugation as described above, and the final pellet was resuspended in PBS. Exosome size and quantity were evaluated using nanoparticle tracking analysis (NTA; NanoSight NS300; Malvern Panalytical) as recommended by the manufacturer. Exosomes were also visualized using transmission electron microscopy (JEM-1400; JEOL).

Gene silencing by shRNA and siRNAs

PKM2 shRNA Lentiviral Particles (Sigma-Aldrich) were used to knock down PKM2 mRNA expression in the PC-3 cell line, and shRNA Lentiviral Particles-A were used as control. Gene knockdown was confirmed using Western blot. Pre-designed siRNA for mouse HIF-1 α and human CXCR4 were obtained from Thermo Fisher Scientific. Mouse HIF-1 α siRNA was used to knock down the target genes in ST2 cells, and human CXCR4 siRNA was used to knock down the target genes in PC3-luc cells following the manufacturer's instructions. Briefly, the cells were transfected with siRNA by using Lipofectamine RNAiMAX (Thermo Fisher Scientific) for 24 h, followed by validation of expected change in expression of the target gene using qPCR.

Real-time PCR

ST2 and MC3T3 cells were processed using standard RNA isolation methods. Briefly, total RNA was extracted using RNeasy Mini Kit (Qiagen), 2 µg of total RNA were reverse transcribed in a final 20-µl volume, and quantitative real-time PCR was performed in triplicate using SYBR Green qPCR MasterMix (Qiagen) in a 10-µl reaction volume on a Roche LightCycler 480 (Roche). The PCR conditions were: 30 cycles at 95°C; followed by 40 cycles at 95°C for 30 s and 65°C for 20 s. Mouse PKM2 primers (cat. no. PPM05100B), mouse CXCL12 primers (cat. no. PPM02965E), mouse BMP-4 primers (cat. no. PPM02996F), and mouse HIF-1 α primers (cat. no. PPM03799C) were purchased from Qiagen. All analyses were performed in triplicate in three independent experiments. Measurements from triplicate threshold cycle (Ct) values were normalized to GAPDH.

Western blot analyses

Exosomes or cells were lysed with radioimmunoprecipitation assay (RIPA) lysis buffer (Millipore) containing a complete protease inhibitor tablet (Sigma-Aldrich). The protein concentration of tumor extracts was determined using bicinchoninic acid (BCA) Protein Assay Kit (Pierce). Lysates were cleared by centrifugation at 14,000 *g* for 20 min. The supernatant fractions were used for Western blot. Protein extracts were resolved by SDS-PAGE and probed with the indicated antibodies. For Western blots, we used antibodies targeting PKM2 (cat. no. 3198S; Cell Signaling), HIF-1 α (cat. no. 14179; Cell Signaling), Alix (cat. no. 2171; Cell Signaling), CD9 (cat. no. sc-13118; Santa Cruz Biotechnology, Inc.), and HSP70 (cat. no. sc-32239; Santa Cruz Biotechnology, Inc.). Antibody-targeting GAPDH (Millipore) was used to visualize GAPDH as a loading control for the Western blots. For the Western blot evaluating human versus mouse PKM2 expression, we used human-specific rabbit polyclonal anti-PKM2 (cat. no. ab85555; Abcam), human-specific mouse monoclonal anti-PKM2 (cat. no. MBS200298; MyBioSource, Inc.), and mouse- and human-reactive rabbit monoclonal anti-PKM2 (cat. no. 3198; Cell Signaling). The antibody binding was revealed using an HRP-conjugated anti-rabbit IgG (1:3,000; Cell Signaling) or anti-mouse IgG (1:3,000; Amersham Pharmacia Biotech). Antibody complexes were detected by SuperSignal West Pico Chemiluminescent Substrate or SuperSignal West Dura Extended Duration Substrate (Thermo Fisher Scientific) and exposure to X-Omat film (Kodak).

CHX inhibition of protein synthesis

The protein synthesis inhibitor CHX was purchased from Sigma-Aldrich and dissolved in DMSO. ST2 cells were incubated with vehicle (DMSO) or with 10 μ g/ml CHX in the presence or absence of PCa exosomes for 24 h. Cell lysates were prepared, and the expression of PKM2 was analyzed by Western blots.

Cytokine qPCR array

Cytokines & Chemokines RT2 Profiler PCR Array (Qiagen) was performed per the manufacturer's instructions. ST2 cells were treated with PCa-Scramble exosomes or PCa-short hairpin PKM2 (PCa-shPKM2) exosomes for 24 h. Total RNA was extracted using Qiagen RNeasy Kit (Qiagen). RT² First Strand Kit (Qiagen) was used for reverse transcription. Real-time PCR was performed with Qiagen SYBR Green Master Mix Kit using a Roche Light Cycler. The array data were analyzed by software in The GeneGlobe Data Analysis Center (Qiagen).

ELISA assays

Mouse CXCL12 levels in supernatants of ST2 cells were analyzed by antibody sandwich ELISA (R&D Systems) following the manufacturer's instructions.

Evaluation of tumor cells seeding bone marrow

After treatments, bone marrow was collected, and Alu-based PCR was performed as previously described (Havens et al., 2008). Briefly, DNA isolation kits were used to prepare genomic DNA from the designated tissues using DNeasy Blood and Tissue Kit (cat. no. 69506; Qiagen, Inc.). All sample

concentrations were standardized in each reaction to exclude false-positive results. Real-time PCRs were performed using 15.0 μ l of TaqMan PCR Master Mix (Applied Biosystems) with 100 nM human Alu TaqMan primers and probe (Forward: 5'-CATGGTGAACCCCGTCTCTA-3'; Reverse: 5'-GCCTCAGCC TCCCGAGTAG-3'; TaqMan probe using a 6-carboxyfluorescein (FAM) fluorophore and a tetramethylrhodamine (TAMRA) quencher: 5'-FAM-ATTAGCCGGGCGTGGTGGCG-TAMRA-3') and 1 μ g of the isolated tissue DNA in a total volume of 30 μ l. The thermal conditions were 50°C for 2 min and 95°C for 10 min followed by 40 cycles of 95°C for 15 s and 60°C for 1 min. The level of expression was detected as an increase in fluorescence using a sequence detection system (ABI PRISM 7700; Applied Biosystems). The DNA levels were expressed as relative copies (% control) normalized against murine β -actin (cat. no. Mm00607939 s1; Thermo Fisher Scientific), and a standard curve constructed from serial dilutions of a purified Alu cDNA fragment was cloned by classic PCR. Numerical data were determined against a standard curve established using mouse BM containing log-fold dilutions of PC-3-ExGFP cells. Pure mouse bone marrow served as a negative control, and human PCa cell line (PC-3-ExGFP) served as a positive control.

Cancer cell growth assay

Cells were seeded in 96-well plates at a density of 2–5 \times 10³ cells in triplicates. After 24 h, cells were treated with different concentrations of the indicated exosomes. The cells were cultured for 3 d, and then the number of viable cells was measured by Cell Proliferation Reagent WST-1 (Roche Applied Science) as directed by the manufacturer.

Invasion assay

The Matrigel invasion assay was performed using BD-Biocoat Invasion Chambers (BD Biosciences) as directed by the manufacturer and previously described (Fu et al., 2003).

Mass spectrometry

The proteins in the SDS-PAGE were digested overnight with sequencing grade-modified trypsin (Promega). Tryptic peptides were resolved on a nanocapillary reverse phase column (Picofrit Column; New Objective) using 1% acetic acid/acetonitrile gradient at 300 nl min⁻¹ and directly infused into a linear ion-trap mass spectrometer (LTQ Orbitrap XL; Thermo Fisher Scientific). The mass spectrometer (MS) was set to collect one survey scan (MS1), followed by MS/MS spectra on the nine most intense ions observed in an MS1 scan. Proteins were identified by searching the data against UniProt Human database appended with decoy (reverse) sequences using X! Tandem/Trans-Proteomic Pipeline software suite. All peptides and proteins with a PeptideProphet and ProteinProphet probability score of >0.9 (false discovery rate [fdr] < 2%) were considered as positive identifications. Proteins found in the control lane were subtracted using an in-house subtraction program, and the remaining were considered as potential interactors.

Exosome treatment of mice

All experimental animals were housed under pathogen-free conditions in accordance with the National Institutes of Health

guidelines, and all animal procedures were approved by the University of Michigan Institutional Animal Care and Use Committee. Male 6- to 8-wk-old severe combined immunodeficient (SCID) mice (strain B6.CB17-Prkdcscid/Szj; Jackson Laboratories) were pretreated via tail vein injection (i.v.) of PCa cell exosomes or exosomes isolated from serum of healthy subjects or PCa patients at 20 μ l (2×10^9 particles) every other day for 5 d, followed by i.c. injection with indicated cell lines, and exosome treatment continued for an additional week. Tumor burden and metastasis were monitored by BLI as indicated.

Orthotopic injection

Male 6- to 8-wk-old SCID mice were anesthetized with isoflurane. The abdomen was surgically prepared with iodine solution. A midline incision was made in the lower abdomen to expose the prostate gland. PC3-luc cells (10^5 cells in 10 μ l) were injected into each dorsal prostate lobe (i.e., both lobes) using an insulin syringe and needle (U-100 30 gauge). The abdominal wound was closed with 6/0 absorbable surgical suture and surgical clips.

Intracardiac (i.c.) injections

The i.c. injections of luciferase-labeled PCa cells were performed in 6- to 8-wk-old male SCID mice (Charles River) under 2.5% isoflurane anesthesia by injecting 10^6 cells suspended in 100 μ l PBS percutaneously into the left cardiac ventricle using a 27-gauge needle. Bioluminescent imaging (BLI) was performed weekly to evaluate for tumor growth.

Implantation of collagen sponges

20 μ l PC3 (2×10^5 cells) or C4-2B cells (1×10^6 cells) were mixed with or without 20 μ l ST2 cells (2×10^5 cells) in mice pretreated with C4-2B exosomes or PC3 exosomes, and were allowed to adsorb into sterile collagen sponges ($3 \times 3 \times 3$ mm³, Gelfoam; Pharmacia & Upjohn Co.). A single mid dorsal incision on the flank of SCID mice was made for the implantation of the collagen sponges with mixed cells and was closed with surgical glue. The animals were monitored twice every week, and tumor volumes were calculated using the following formula: $V = (\text{the shortest diameter})^2 \times (\text{the longest diameter})$.

AMD3100 treatment

AMD3100 was purchased from Sigma-Aldrich. For proliferation and invasion assay, PC3 cells were exposed to exosomes from C4-2B cells with or without 30 μ M AMD3100, exosomes from C4-2B cells transduced with scramble, PKM2-shRNA plus/minus 30 μ M AMD3100, or control media for 48 h. For determining the seeding of PC3 cells in mouse bone marrow, SCID mice (6–8 wk old) were pretreated with AMD3100 (5 mg/kg, 100 μ l, i.p. injection, daily) or vehicle (0.9% saline) with or without i.v. injection of C4-2B exosomes at 20 μ l every other day for 5 d ($n = 5$ /group), followed by i.c. injection of PC3 cells (2×10^5 cells). Mice were sacrificed 24 h later, and the bone marrows from mouse femurs and tibia were collected and stored at -80°C . The number of disseminated PC3 cells was assessed by qPCR using human Alu primer. For determining the PC3 tumor burden and metastasis in SCID mice, SCID mice (6–8 wk old) were

pretreated with AMD3100 (5 mg/kg, 100 μ l, i.p. injection, daily) or vehicle (0.9% saline) with or without i.v. injection of C4-2B exosomes at 20 μ l every other day for 5 d ($n = 10$ /group), followed with i.c. injection of PC3-luc cells or PC3-luc cells treated with small interfering RNA (siRNA); namely, siCXCR4 or si-Control (2×10^5 cells). Exosome treatment was continued for one additional week. The tumor burden and metastasis were monitored by BLI 4 wk after PC3-luc cell injection.

BLI in vivo

Mice were injected i.p. with luciferin (100 μ l at 40 mg/ml in PBS) before imaging. Mice were anesthetized with 1.5% isoflurane/air and the Xenogen IVIS cryogenically cooled imaging system. Bioluminescence generated by the luciferin/luciferase reaction served as a locator for cancer growth and was used for quantification using the LivingImage software on a red (high intensity/cell number) to blue (low intensity/cell number) visual scale. A digital grayscale animal image was acquired followed by acquisition and overlay of a pseudocolor image representing the spatial distribution of detected photon counts emerging from active luciferase within the animal. Signal intensity was quantified as the sum of all detected photons within the region of interest during a 1-min luminescent integration time.

Evaluation for GFP-positive exosomes in tissue

To determine the in vivo distribution of exosomes, we created a PCa cell line that has GFP-labeled exosomes so that we could track the exosomes in vivo. Specifically, PC3 cells were stably transduced with CD63-GFP (pCT-CD-63-GFP; System Biosciences) followed by puromycin selection. CD63 is tetraspanin, which is incorporated into exosomes. In some cases, GFP⁺ exosomes were injected into the tail vein of mice, and after 24 h, the femur and tibiae were flushed with trypsin to collect the bone marrow, and liver and lungs were also collected. Tissues (27-mm³ sections) were subjected to trypsinization, and cells were resuspended after washing in 10% FBS in PBS at 10^5 /ml. Cells were then subjected to fluorescent imaging to evaluate for presence of GFP⁺ exosomes. To determine if primary tumor exosomes target the marrow microenvironment, we injected PC-3-ExGFP into murine prostate dorsal lobes. After 3 wk, we harvested marrow as above and subjected it to fluorescence.

Statistical analyses

Numerical data are expressed as mean \pm SD of the mean. All in vitro experiments were performed between two and four times. Statistical significance was tested using Student's *t* test for two groups or ANOVA and Fisher's least significant difference for post-hoc analysis when three or more groups were present. Statistical significance was determined at $P \leq 0.05$. Microsoft Excel (Microsoft) and GraphPad Prism software (GraphPad Software) were used for statistical analysis.

Online supplemental material

Fig. S1 shows that PCa-derived exosomes promote tumor growth in mouse bone but have no direct effect on cell growth in vitro. Fig. S2 shows that PCa exosomes educate bone marrow

cells to promote PCa growth. Fig. S3 shows that PCa-derived exosomes increase PKM2 expression in stromal cells. Fig. S4 shows that PCa exosomes promote PCa tumor growth through CXCL12 from bone marrow cells induced by PKM2. Fig. S5 shows that PCa exosomes increase CXCL12 production in BMSCs through HIF-1 α induced by PKM2.

Acknowledgments

We thank Dr. Renny Franceschi for providing MC3T3-E1 cells.

This work was supported by National Institutes of Health grant R01 CA093900.

The authors declare no competing financial interests.

Author contributions: J. Dai, experimental design, experimental procedures, and manuscript preparation; J. Escara-Wilke, experimental procedures; J.M. Keller, experimental procedures and manuscript preparation; Y. Jung, experimental procedures; R.S. Taichman, experimental design and manuscript preparation; K.J. Pienta, experimental design and manuscript preparation; and E.T. Keller, experimental design and manuscript preparation.

Submitted: 24 January 2019

Revised: 30 June 2019

Accepted: 3 September 2019

References

Azoitei, N., A. Becher, K. Steinestel, A. Rouhi, K. Diepold, F. Genze, T. Simmet, and T. Seufferlein. 2016. PKM2 promotes tumor angiogenesis by regulating HIF-1 α through NF- κ B activation. *Mol. Cancer*. 15:3. <https://doi.org/10.1186/s12943-015-0490-2>

Camussi, G., M.C. Deregiibus, S. Bruno, C. Grange, V. Fonsato, and C. Tetta. 2011. Exosome/microvesicle-mediated epigenetic reprogramming of cells. *Am. J. Cancer Res.* 1:98–110.

Ceradini, D.J., A.R. Kulkarni, M.J. Callaghan, O.M. Tepper, N. Bastidas, M.E. Kleinman, J.M. Capla, R.D. Galiano, J.P. Levine, and G.C. Gurtner. 2004. Progenitor cell trafficking is regulated by hypoxic gradients through HIF-1 induction of SDF-1. *Nat. Med.* 10:858–864. <https://doi.org/10.1038/nm1075>

Chao, T.K., T.S. Huang, Y.P. Liao, R.L. Huang, P.H. Su, H.Y. Shen, H.C. Lai, and Y.C. Wang. 2017. Pyruvate kinase M2 is a poor prognostic marker of and a therapeutic target in ovarian cancer. *PLoS One*. 12:e0182166. <https://doi.org/10.1371/journal.pone.0182166>

Chen, M., J. Zhang, and J.L. Manley. 2010. Turning on a fuel switch of cancer: hnRNP proteins regulate alternative splicing of pyruvate kinase mRNA. *Cancer Res.* 70:8977–8980. <https://doi.org/10.1158/0008-5472.CAN-10-2513>

Costa-Silva, B., N.M. Aiello, A.J. Ocean, S. Singh, H. Zhang, B.K. Thakur, A. Becker, A. Hoshino, M.T. Mark, H. Molina, et al. 2015. Pancreatic cancer exosomes initiate pre-metastatic niche formation in the liver. *Nat. Cell Biol.* 17:816–826. <https://doi.org/10.1038/ncb3169>

Croner, L.J., R. Dillon, A. Kao, S.N. Kairs, R. Benz, I.J. Christensen, H.J. Nielsen, J.E. Blume, and B. Wilcox. 2017. Discovery and validation of a colorectal cancer classifier in a new blood test with improved performance for high-risk subjects. *Clin. Proteomics*. 14:28. <https://doi.org/10.1186/s12014-017-9163-z>

Desai, S., M. Ding, B. Wang, Z. Lu, Q. Zhao, K. Shaw, W.K. Yung, J.N. Weinstein, M. Tan, and J. Yao. 2014. Tissue-specific isoform switch and DNA hypomethylation of the pyruvate kinase PKM gene in human cancers. *Oncotarget*. 5:8202–8210. <https://doi.org/10.18632/oncotarget.1159>

Di Vizio, D., M. Morello, A.C. Dudley, P.W. Schow, R.M. Adam, S. Morley, D. Mulholland, M. Rotinen, M.H. Hager, L. Insabato, et al. 2012. Large oncosomes in human prostate cancer tissues and in the circulation of mice with metastatic disease. *Am. J. Pathol.* 181:1573–1584. <https://doi.org/10.1016/j.ajpath.2012.07.030>

Dong, G., Q. Mao, W. Xia, Y. Xu, J. Wang, L. Xu, and F. Jiang. 2016. PKM2 and cancer: The function of PKM2 beyond glycolysis. *Oncol. Lett.* 11: 1980–1986. <https://doi.org/10.3892/ol.2016.4168>

Dragomir, M., B. Chen, and G.A. Calin. 2018. Exosomal lncRNAs as new players in cell-to-cell communication. *Transl. Cancer Res.* 7(Suppl 2): S243–S252. <https://doi.org/10.21037/tcr.2017.10.46>

Esposito, M., T. Guise, and Y. Kang. 2018. The biology of bone metastasis. *Cold Spring Harb. Perspect. Med.* 8:a031252. <https://doi.org/10.1101/cshperspect.a031252>

Fu, Z., P.C. Smith, L. Zhang, M.A. Rubin, R.L. Dunn, Z. Yao, and E.T. Keller. 2003. Effects of raf kinase inhibitor protein expression on suppression of prostate cancer metastasis. *J. Natl. Cancer Inst.* 95:878–889. <https://doi.org/10.1093/jnci/95.12.878>

Fujita, K., and N. Nonomura. 2018. Urinary biomarkers of prostate cancer. *Int. J. Urol.* 25:770–779. <https://doi.org/10.1111/iju.13734>

Fung, K.Y., B. Tabor, M.J. Buckley, I.K. Priebe, L. Purins, C. Pompeia, G.V. Brierley, T. Lockett, P. Gibbs, J. Tie, et al. 2015. Blood-based protein biomarker panel for the detection of colorectal cancer. *PLoS One*. 10: e0120425. <https://doi.org/10.1371/journal.pone.0120425>

Ge, R., E. Tan, S. Sharghi-Namini, and H.H. Asada. 2012. Exosomes in cancer microenvironment and beyond: Have we overlooked these extracellular messengers? *Cancer Microenviron.* 5:323–332. <https://doi.org/10.1007/s12307-012-0110-2>

Havens, A.M., E.A. Pedersen, Y. Shiozawa, C. Ying, Y. Jung, Y. Sun, C. Neeley, J. Wang, R. Mehra, E.T. Keller, et al. 2008. An in vivo mouse model for human prostate cancer metastasis. *Neoplasia*. 10:371–380. <https://doi.org/10.1593/neo.08154>

Hood, J.L., R.S. San, and S.A. Wickline. 2011. Exosomes released by melanoma cells prepare sentinel lymph nodes for tumor metastasis. *Cancer Res.* 71: 3792–3801. <https://doi.org/10.1158/0008-5472.CAN-10-4455>

Huang, C., Z. Huang, P. Bai, G. Luo, X. Zhao, and X. Wang. 2018. Expression of pyruvate kinase M2 in human bladder cancer and its correlation with clinical parameters and prognosis. *Oncotargets Ther.* 11:2075–2082. <https://doi.org/10.2147/OTT.S152999>

Iqbal, M.A., V. Gupta, P. Gopinath, S. Mazurek, and R.N. Bamezai. 2014. Pyruvate kinase M2 and cancer: An updated assessment. *FEBS Lett.* 588: 2685–2692. <https://doi.org/10.1016/j.febslet.2014.04.011>

Jella, K.K., T.H. Nasti, Z. Li, S.R. Malla, Z.S. Buchwald, and M.K. Khan. 2018. Exosomes, their biogenesis and role in inter-cellular communication, tumor microenvironment and cancer immunotherapy. *Vaccines (Basel)*. 6:e69.

Lee, J., M.H. Kwon, J.A. Kim, and W.J. Rhee. 2018. Detection of exosome miRNAs using molecular beacons for diagnosing prostate cancer. *Artif. Cells Nanomed. Biotechnol.* 46(sup3):S52–S63. <https://doi.org/10.1080/21691401.2018.1489263>

Loh, S.A., E.I. Chang, M.G. Galvez, H. Thangarajah, S. El-ftesi, I.N. Vial, D.A. Lin, and G.C. Gurtner. 2009. SDF-1 α expression during wound healing in the aged is HIF dependent. *Plast. Reconstr. Surg.* 123(2 Suppl):65S–75S. <https://doi.org/10.1097/PRS.0b013e318191bdf4>

Lu, H., N. Bowler, L.A. Harshyne, D. Craig Hooper, S.R. Krishn, S. Kurtoglu, C. Fedele, Q. Liu, H.Y. Tang, A.V. Kossenkov, et al. 2018. Exosomal α v β 6 integrin is required for monocyte M2 polarization in prostate cancer. *Matrix Biol.* 70:20–35. <https://doi.org/10.1016/j.matbio.2018.03.009>

Luo, W., and G.L. Semenza. 2011. Pyruvate kinase M2 regulates glucose metabolism by functioning as a coactivator for hypoxia-inducible factor 1 in cancer cells. *Oncotarget*. 2:551–556. <https://doi.org/10.18632/oncotarget.299>

Martin, S.K., P. Diamond, S.A. Williams, L.B. To, D.J. Peet, N. Fujii, S. Gronthos, A.L. Harris, and A.C. Zannettino. 2010. Hypoxia-inducible factor-2 is a novel regulator of aberrant CXCL12 expression in multiple myeloma plasma cells. *Haematologica*. 95:776–784. <https://doi.org/10.3324/haematol.2009.015628>

Mathivanan, S., H. Ji, and R.J. Simpson. 2010. Exosomes: Extracellular organelles important in intercellular communication. *J. Proteomics*. 73: 1907–1920. <https://doi.org/10.1016/j.jprot.2010.06.006>

Mohammad, G.H., S.W. Olde Damink, M. Malago, D.K. Dhar, and S.P. Pereira. 2016. Pyruvate kinase M2 and lactate dehydrogenase A are overexpressed in pancreatic cancer and correlate with poor outcome. *PLoS One*. 11:e0151635. <https://doi.org/10.1371/journal.pone.0151635>

Ortiz, A., and S.H. Lin. 2012. Osteolytic and osteoblastic bone metastases: Two extremes of the same spectrum? *Recent Results Cancer Res.* 192:225–233. https://doi.org/10.1007/978-3-642-21892-7_11

Paget, S. 1889. The distribution of secondary growth in cancer of the breast. *Lancet*. 133:571–573. [https://doi.org/10.1016/S0140-6736\(00\)49915-0](https://doi.org/10.1016/S0140-6736(00)49915-0)

- Panigrahi, G.K., A. Ramteke, D. Birks, H.E. Abouzeid Ali, S. Venkataraman, C. Agarwal, R. Vibhakar, L.D. Miller, R. Agarwal, Z.Y. Abd Elmaged, et al. 2018. Exosomal microRNA profiling to identify hypoxia-related biomarkers in prostate cancer. *Oncotarget*. 9:13894–13910. <https://doi.org/10.18632/oncotarget.24532>
- Papachristou, D.J., E.K. Basdra, and A.G. Papavassiliou. 2012. Bone metastases: Molecular mechanisms and novel therapeutic interventions. *Med. Res. Rev.* 32:611–636. <https://doi.org/10.1002/med.20224>
- Peinado, H., M. Alečković, S. Lavotshkin, I. Matei, B. Costa-Silva, G. Moreno-Bueno, M. Hergueta-Redondo, C. Williams, G. García-Santos, C. Ghajar, et al. 2012. Melanoma exosomes educate bone marrow progenitor cells toward a pro-metastatic phenotype through MET. *Nat. Med.* 18:883–891. <https://doi.org/10.1038/nm.2753>
- Ren, G., M. Esposito, and Y. Kang. 2015. Bone metastasis and the metastatic niche. *J. Mol. Med. (Berl.)*. 93:1203–1212. <https://doi.org/10.1007/s00109-015-1329-4>
- Roato, I., P. D'Amelio, E. Gorassini, A. Grimaldi, L. Bonello, C. Fiori, L. Delsedime, A. Tizzani, A. De Libero, G. Isaia, et al. 2008. Osteoclasts are active in bone forming metastases of prostate cancer patients. *PLoS One*. 3:e3627. <https://doi.org/10.1371/journal.pone.0003627>
- Rzechonek, A., A. Kaminska, P. Mamczur, A. Drapiewski, and W. Budzynski. 2017. Limited clinical significance of dimeric form of pyruvate kinase as a diagnostic and prognostic biomarker in non-small cell lung cancer. *Adv. Exp. Med. Biol.* 955:51–57. https://doi.org/10.1007/5584_2016_92
- Sabbota, A.L., H.R. Kim, X. Zhe, R. Fridman, R.D. Bonfil, and M.L. Cher. 2010. Shedding of RANKL by tumor-associated MT1-MMP activates Src-dependent prostate cancer cell migration. *Cancer Res.* 70:5558–5566. <https://doi.org/10.1158/0008-5472.CAN-09-4416>
- Semenza, G.L. 2011. Regulation of metabolism by hypoxia-inducible factor 1. *Cold Spring Harb. Symp. Quant. Biol.* 76:347–353. <https://doi.org/10.1101/sqb.2011.76.010678>
- Shah, R.B., R. Mehra, A.M. Chinnaiyan, R. Shen, D. Ghosh, M. Zhou, G.R. Macvicar, S. Varambally, J. Harwood, T.A. Bismar, et al. 2004. Androgen-independent prostate cancer is a heterogeneous group of diseases: Lessons from a rapid autopsy program. *Cancer Res.* 64:9209–9216. <https://doi.org/10.1158/0008-5472.CAN-04-2442>
- Shiozawa, Y., E.A. Pedersen, A.M. Havens, Y. Jung, A. Mishra, J. Joseph, J.K. Kim, L.R. Patel, C. Ying, A.M. Ziegler, et al. 2011. Human prostate cancer metastases target the hematopoietic stem cell niche to establish footholds in mouse bone marrow. *J. Clin. Invest.* 121:1298–1312. <https://doi.org/10.1172/JCI143414>
- Shupp, A.B., A.D. Kolb, D. Mukhopadhyay, and K.M. Bussard. 2018. Cancer metastases to bone: Concepts, mechanisms, and interactions with bone osteoblasts. *Cancers (Basel)*. 10:e182. <https://doi.org/10.3390/cancers10060182>
- Sun, Y.X., J. Wang, C.E. Shelburne, D.E. Lopatin, A.M. Chinnaiyan, M.A. Rubin, K.J. Pienta, and R.S. Taichman. 2003. Expression of CXCR4 and CXCL12 (SDF-1) in human prostate cancers (PCa) in vivo. *J. Cell. Biochem.* 89:462–473. <https://doi.org/10.1002/jcb.10522>
- Suva, L.J., C. Washam, R.W. Nicholas, and R.J. Griffin. 2011. Bone metastasis: Mechanisms and therapeutic opportunities. *Nat. Rev. Endocrinol.* 7:208–218. <https://doi.org/10.1038/nrendo.2010.227>
- Taichman, R., L. McCauley, and N. Taichman. 2000. Use of the SDF-1/CXCR4 pathway in prostate cancer metastasis to bone. *Blood*. 96:571a.
- Taichman, R.S., C. Cooper, E.T. Keller, K.J. Pienta, N.S. Taichman, and L.K. McCauley. 2002. Use of the stromal cell-derived factor-1/CXCR4 pathway in prostate cancer metastasis to bone. *Cancer Res.* 62:1832–1837.
- Tamada, M., M. Suematsu, and H. Saya. 2012. Pyruvate kinase M2: Multiple faces for conferring benefits on cancer cells. *Clin. Cancer Res.* 18:5554–5561. <https://doi.org/10.1158/1078-0432.CCR-12-0859>
- Taylor, D.D., and C. Gercel-Taylor. 2011. Exosomes/microvesicles: Mediators of cancer-associated immunosuppressive microenvironments. *Semin. Immunopathol.* 33:441–454. <https://doi.org/10.1007/s00281-010-0234-8>
- Théry, C., K.W. Witwer, E. Aikawa, M.J. Alcaraz, J.D. Anderson, R. Andriantsitohaina, A. Antoniou, T. Arab, F. Archer, G.K. Atkin-Smith, et al. 2018. Minimal information for studies of extracellular vesicles 2018 (MISEV2018): A position statement of the International Society for Extracellular Vesicles and update of the MISEV2014 guidelines. *J. Extracell. Vesicles*. 7:1535750. <https://doi.org/10.1080/20013078.2018.1535750>
- Valentino, A., P. Reclusa, R. Sirera, M. Giallombardo, C. Camps, P. Pauwels, S. Crispi, and C. Rolfo. 2017. Exosomal microRNAs in liquid biopsies: Future biomarkers for prostate cancer. *Clin. Transl. Oncol.* 19:651–657. <https://doi.org/10.1007/s12094-016-1599-5>
- Wang, H.J., Y.J. Hsieh, W.C. Cheng, C.P. Lin, Y.S. Lin, S.F. Yang, C.C. Chen, Y. Izumiya, J.S. Yu, H.J. Kung, et al. 2014. JMJD5 regulates PKM2 nuclear translocation and reprograms HIF-1 α -mediated glucose metabolism. *Proc. Natl. Acad. Sci. USA*. 111:279–284. <https://doi.org/10.1073/pnas.1311249111>
- Wang, Y.H., J. Ji, B.C. Wang, H. Chen, Z.H. Yang, K. Wang, C.L. Luo, W.W. Zhang, F.B. Wang, and X.L. Zhang. 2018. Tumor-derived exosomal long noncoding RNAs as promising diagnostic biomarkers for prostate cancer. *Cell. Physiol. Biochem.* 46:532–545. <https://doi.org/10.1159/000488620>
- Wani, S., D. Kaul, R.S. Mavuduru, N. Kakkar, and A. Bhatia. 2017. Urinary-exosomal miR-2909: A novel pathognomonic trait of prostate cancer severity. *J. Biotechnol.* 259:135–139. <https://doi.org/10.1016/j.jbiotec.2017.07.029>
- Warner, S.L., K.J. Carpenter, and D.J. Bearss. 2014. Activators of PKM2 in cancer metabolism. *Future Med. Chem.* 6:1167–1178. <https://doi.org/10.4155/fmc.14.70>
- Yang, W., and Z. Lu. 2013. Nuclear PKM2 regulates the Warburg effect. *Cell Cycle*. 12:3154–3158. <https://doi.org/10.4161/cc.26182>
- Ye, Y., S.L. Li, Y.Y. Ma, Y.J. Diao, L. Yang, M.Q. Su, Z. Li, Y. Ji, J. Wang, L. Lei, et al. 2017. Exosomal miR-141-3p regulates osteoblast activity to promote the osteoblastic metastasis of prostate cancer. *Oncotarget*. 8:94834–94849. <https://doi.org/10.18632/oncotarget.22014>
- Yoneda, T., and T. Hiraga. 2005. Crosstalk between cancer cells and bone microenvironment in bone metastasis. *Biochem. Biophys. Res. Commun.* 328:679–687. <https://doi.org/10.1016/j.bbrc.2004.11.070>
- Zhang, J., J. Dai, Y. Qi, D.L. Lin, P. Smith, C. Strayhorn, A. Mizokami, Z. Fu, J. Westman, and E.T. Keller. 2001. Osteoprotegerin inhibits prostate cancer-induced osteoclastogenesis and prevents prostate tumor growth in the bone. *J. Clin. Invest.* 107:1235–1244. <https://doi.org/10.1172/JCI11685>
- Zhu, H., H. Luo, X. Zhu, X. Hu, L. Zheng, and X. Zhu. 2017. Pyruvate kinase M2 (PKM2) expression correlates with prognosis in solid cancers: A meta-analysis. *Oncotarget*. 8:1628–1640.